these therapeutic options, ARBs are initially expected to suppress the development of hepatic fibrosis in NASH. Hepatic stellate cell (HSC), which is a major fibrogenic cell type in the liver and also contributes to hepatic inflammation through induction of cytokines, expresses AT1R, and blockade of Ang II signaling markedly attenuates hepatic inflammation and fibrosis in experimental models of chronic liver fibrosis [8,9]. A clinical report has also demonstrated that losartan, an ARB, improved hepatic necroinflammation and fibrosis in NASH patients [10].

In addition to anti-fibrotic/inflammatory effect, emerging data have suggested that ARBs improve glucose and lipid metabolism. In a large clinical trial, losartan substantially lowered the risk for type 2 diabetes compared with other antihypertensive therapies [11]. An animal study using obese Zucker rats has also demonstrated that high dose of irbesartan improved insulin sensitivity [12]. More recently, it has been shown that telmisartan, unlike other ARBs improved the development of hepatic steatosis in animal models [7,13,14]. These metabolic effects of ARBs might be explained in part by the *in vitro* study, in which a distinct subtype of ARBs induced transcriptional activities of peroxisome proliferator-activated receptor (PPAR) γ, independent of their AT1R blocking actions [15,16]. However, it is noteworthy that PPARγ-activating potency by ARBs appears rather modest as determined by transcription reporter assays, with median effective concentration (EC_{50}) of telmisartan, the most potent PPARγ activator among ARBs, 5.02 μmol/L compared to 0.2 μmol/L of pioglitazone, a full agonist of PPARγ [15,16]. Interestingly, treatment with olmesartan, which has no impact on PPARγ activation, has been proved to attenuate the development of hepatic steatosis, suggesting the possibility that the blockade of AT1R itself might contribute to hepatic lipid homeostasis [17]. To further investigate the direct role for AT1R in hepatic steatosis, we applied two different approaches: (1) animal model of steatohepatitis using mice lacking AT1aR ($AT1a^{-/-}$), which is the only Ang II receptor subtype expressed in rodent liver, and (2) *in vitro* cellular steatosis model in which gene silencing by RNA interference targeting AT1R was performed [18]. Our data demonstrated reduced lipid accumulation in the absence of AT1R with significant induction of PPARα. Apart from PPARγ modulating action of ARBs, these data support the potential efficacy of AT1R blockade in the treatment of NAFLD/NASH.

2. Materials and methods

2.1. Animal

$AT1a^{-/-}$ mice were provided by Mitsubishi Tanabe Pharma (Osaka, Japan) and C57BL/6 mice were obtained from Charles River Laboratories (Yokohama, Japan) [19]. Both strains of the mice have the same genetic background. The mice were housed in a standard 12 h light/dark cycle facility, and fed either standard chow diet or methionine–choline deficient (MCD) diet (Oriental Yeast Co., Tokyo, Japan) for 8 weeks with free access to drinking water. Male mice at 6–8 weeks of age were used in this study, and all animal procedures were performed according to the guidelines of Institute of Laboratory Animal Science, Hiroshima University.

2.2. Histological examination

Liver samples were fixed in 4% formaldehyde solution, embedded in paraffin, and cut into 5 μm-thick sections. Staining for hematoxylin and eosin (H-E) or Azan-Mallory was carried out with standard techniques.

2.3. Analytical techniques

Serum triglyceride (TG) concentration was determined enzymatically using a Triglyceride E-test (Wako Chemicals, Osaka, Japan). To quantify hepatic TG content, hepatic lipid was extracted as previously described by Bligh and Dyer and subjected to the same procedure as serum assay followed by the standardization of protein concentrations [20]. Hepatic thiobarbituric acid-reactive substances (TBARS) levels were quantified using an OXI-TEK TBARS Assay Kit (Zeprometrix Corporation, New York) with protein standardization. Serum TBARS levels were assayed using the same kit. β-Hydroxybutyrate was assayed using an assay kit (BioVision, Mountain View, CA). The activities of serum transaminases were determined enzymatically.

2.4. Cell culture and gene silencing by small interfering RNA (siRNA)

HepG2 cells (human hepatoma cell line) were cultured in Dulbecco's modified Eagle's medium supplemented with 10% (v/v) fetal bovine serum. For gene silencing, two different sequences of small interfering RNA (siRNA) targeting human AT1R were purchased from Sigma–Aldrich (siRNA ID: SASI_Hs01_00206672, SASI_Hs02_00206672). Cells were transfected using Lipofectamine RNAiMAX (Invitrogen) in 6-well plates containing 2.5×10^5 cells in each well with 10 nM of siRNA duplex. siPerfect Negative Controls (Sigma–Aldrich) was utilized as a negative control siRNA. In the preliminary experiment, siRNA duplex of SASI_Hs02_00206672 effectively knocked down AT1R expression compared to SASI_Hs01_00206672, and this was used for the following experiments. After 24 and 48 h of transfection, cells were subjected to gene quantification by real-time PCR and *in vitro* steatosis experiment, respectively.

2.5. In vitro model of cellular steatosis

Palmitic acid (C16:0) and oleic acid (C18:1) (Sigma, St. Louis, MO) were dissolved in isopropanol to obtain 20 or 40 mM stock mixture solution (2:1 oleate: palmitate), and the concentration of vehicle was 1% in final incubations [21]. Telmisartan (provided by Boehringer Ingelheim, Germany) was resolved in dimethyl sulfoxide (DMSO) to obtain 10 mM stock solution. To investigate the effect of telmisartan on cellular steatosis, cells were exposed to 200 or 400 μM of free fatty acids (FFAs) mixture with or without 2 h preincubation of 10 μM telmisartan. To assess the influence of AT1R knockdown on cellular steatosis, cells were treated with FFAs after 48 h of siRNA transfection. Following 24 h of incubation with FFAs, cells were subjected to determination of cellular lipid content by Nile Red assay and β-hydroxybutyrate levels in the media.

2.6. Nile Red assay

The lipid content in cultured cells was quantified fluorometrically using Nile Red, a vital lipophilic dye as previously described [22].

Briefly, cell monolayers were washed twice with phosphate buffered saline (PBS) followed by fixation with 4% formaldehyde solution for 15 min, and washed with PBS twice again. Cells were stained for 30 min with Nile Red solution at a final concentration of 200 μg/ml in PBS. Monolayers were washed thereafter with PBS and measured fluorometorically (excitation; 488 nm. emission; 550 nm) [23].

2.7. Quantitative real-time PCR

Total RNA was isolated using RNeasy Mini Kit (Qiagen, Germany). cDNA was synthesized from 1 μg of total RNA with GeneAmp Gold RNA PCR Core Kit (Applied Biosystems, Foster City, CA). To quantify AT1R mRNA expression in human heart and kidney, PCR Ready First Strand cDNA (BioChain, Hayward, CA) was utilized. Specific primers except AT1R from PrimerBank, a public resource for PCR primers (http://pga.mgh.harvard.edu/primerbank/, ID: 14043066) were designed using Primer3 (http://frodo.wi.mit.edu) with nucleotide sequences from GenBank™ as listed in Table 1. Real-time PCR was carried out with Lightcycler 1.5 system using Lightcycler FastStart DNA Master plus SYBR Green I (Roche Applied Science). The relative expression levels were calculated with the formula $2^{-\Delta C_t}$, where ΔC_t is the difference in threshold cycle (C_t) values between target gene and ribosomal protein S18 as a control.

2.8. Western blot analysis for AT1R

Fifty microgram of protein prepared from HepG2 cells using RIPA buffer supplemented with protease inhibitors (Roche Diagnostics), as well as Total Protein-Human Adult Normal Tissues (Biochain, Hayward, CA) were fractionated by SDS–PAGE and subjected to Western blot analysis using rabbit polyclonal antibodies against human AT1R (N-10) (Santa Cruz Biotechnology, Santa Cruz, CA). The blots were visualized by enhanced chemiluminescence.

2.9. Statistical analysis

The data are expressed as the means ± SE. The statistical analysis was performed using Student's t test, and differences were considered statistically significant for a two-tailed $p < 0.05$.

3. Results

3.1. Mice lacking AT1R are resistant to steatohepatitis

MCD diet has been reported to cause steatohepatitis which represents most of histological features of human NASH [24,25]. As shown in Fig. 1A, histological analysis of the livers demonstrated that MCD diet for 8 weeks resulted in apparent steatosis with inflammatory cell infiltration mainly in portal area in wild-type (WT) mice. However, in contrast to WT mice, $AT1a^{-/-}$ mice displayed no significant changes in the liver (Fig. 1A, right panel). Azan-Mallory staining of the liver from WT mice revealed mild pericellular fibrosis, which was absent in $AT1a^{-/-}$ mice (Fig. 1A, lower panels). In accordance with these histological observations, hepatic TG content increased by 3-fold in WT and remained no significant 1.5-fold increase in $AT1a^{-/-}$ mice following 8 weeks of MCD diet (Fig. 1B, left panel). Serum TG level following MCD diet was reduced in both genetic groups with more drastic change in WT mice (Fig. 1B, right panel). The substantial changes in hepatic TG content suggested the possibility that the expression of PPARα, a central player in hepatic lipid metabolism, might be influenced by AT1aR expression. This was assessed by quantitative real-time PCR. While MCD diet did not affect hepatic PPARα expression in both genetic strains, absence of AT1aR was associated with significant 3-fold increase in PPARα mRNA in chow diet-fed mice (Fig. 1C). Since PPARα mediates hepatic expression of genes regulating lipid oxidation, we next assessed serum level of β-hydroxybutyrate, an end product of hepatic fatty acid oxidation. Fig. 1D demonstrates 3-fold increase in serum β-hydroxybutyrate in $AT1a^{-/-}$ mice compared to WT mice following MCD diet. This might be a potential explanation for reduced hepatic lipid accumulation in $AT1a^{-/-}$ mice.

3.2. Lack of AT1R ameliorates liver injury

As shown in Fig. 2, there were no differences in aspartate aminotransferase (AST) and alanine aminotrasferase (ALT) levels between WT and $AT1a^{-/-}$ mice when fed chow diet. MCD diet caused significant increase in AST and ALT levels in WT mice, whereas there was no significant increase of these liver enzymes in $AT1a^{-/-}$ mice.

Table 1
Primer used for quantitative real-time PCR.

Gene	Forward	Reverse	GenBank Accession No.
mPPARα	tgcaaacttggacttgaacg	tgatgtcacagaacggcttc	BC016892
AT1	atccaagatgattgtcccaaagc	gcccatagtggcaaagtcagtaa	
PPARα	cagtggagcattgaacatcg	gttgtgtgacatcccgacag	NM_001001928
ApoB100	agccttgctgaagaaaacca	atgcccctcttgatgttcag	M14162
ASCL1	ccagaagggcttcaagactg	gccttctctggcttgtcaac	NM_001995
RPS18	atagcctttgccatcactgc	ggacctggctgtatttttcca	NM_022551
PPARγ	atcaaagtggagcctgcatc	acccttgcatccttcacaag	NM_138711
PPARβ(δ)	ctatccgttttggtcggatg	cgatgtcgtggatcacaaag	NM_006238

mPPARα, mouse peroxisome proliferator-activated receptor α; AT1, angiotensin II type I receptor; PPAR, human PPAR; ApoB100, apolipoprotein B-100; ACSL1, acyl-CoA synthetase long-chain family member 1; RPS18, ribosomal protein S18.

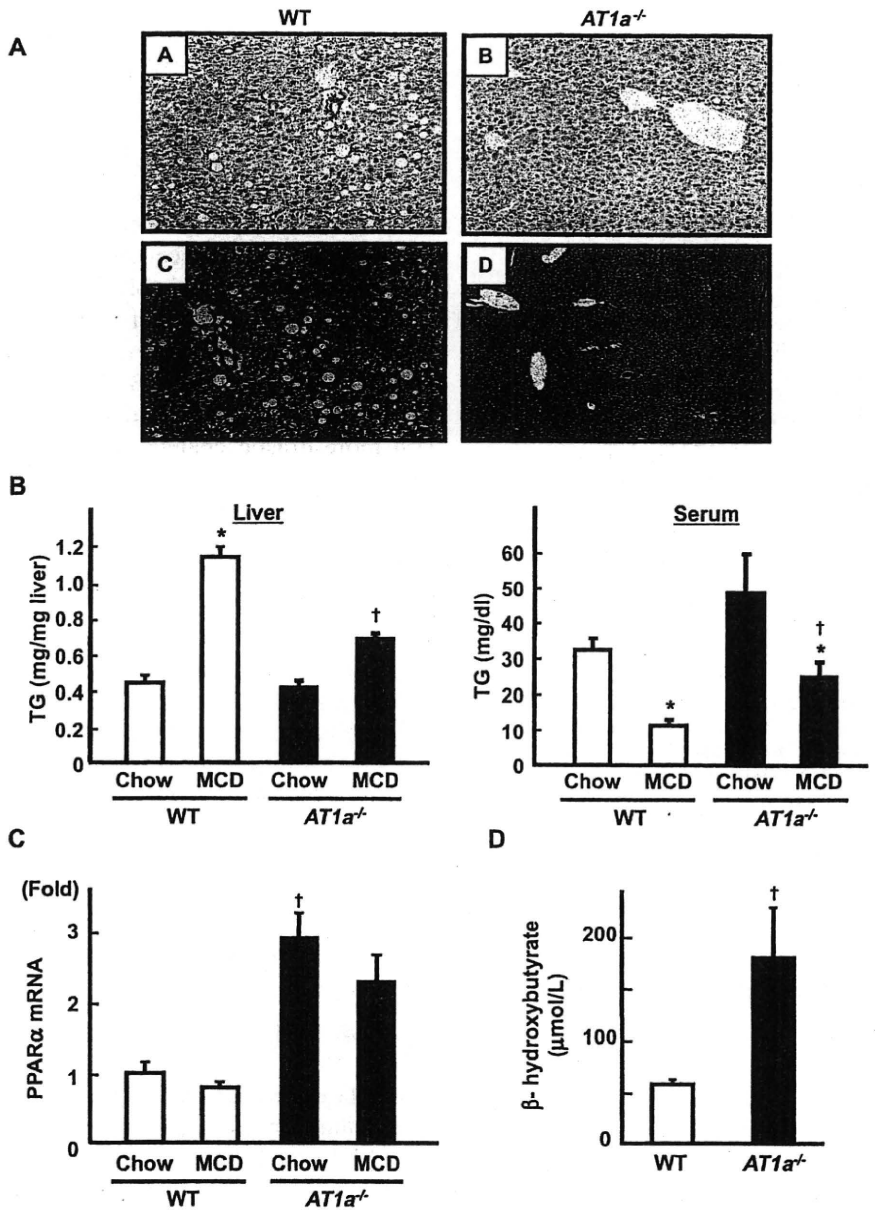

Fig. 1. The absence of AT1aR expression attenuates the development of MCD diet-induced hepatic steatosis in mice. (A) Liver sections from MCD diet-fed WT (A and C) and $AT1a^{-/-}$ mice (B and D) were processed for haematoxylin & eosin (HE) (upper panels) or Azan-Mallory staining (lower panels). Hepatic steatosis as well as fibrosis are evident only in WT mice (original magnification 100×). (B) TG concentrations in liver (left panel) and serum (right panel) obtained from WT (open bars) and $AT1a^{-/-}$ (closed bars) mice (n = 6/each group) were determined after feeding either normal chow or MCD diet. (C) Hepatic PPARα mRNA expression was quantified (n = 5/each group) by quantitative real-time PCR. (D) The serum level of β-hydroxybutyrate in WT (n = 5) and $AT1a^{-/-}$(n = 6) mice fed MCD diet was determined. $^{*}p < 0.05$, chow-fed vs. MCD diet-fed mice. $^{\dagger}p < 0.05$, WT vs. $AT1a^{-/-}$ mice. [This figure appears in colour on the web.]

3.3. Influence of AT1R expression on oxidative stress

Since lipid peroxidation product plays an important role as a "2nd hit" in the pathogenesis of NASH, we next examined serum and hepatic levels of TBARS [26]. Fig. 3 demonstrates marked increase in TBARS levels in serum and liver of WT mice following MCD diet. In contrast, $AT1a^{-/-}$ mice showed no significant changes in TBARS levels, which presumably reflected the reduction of liver injury as demonstrated in AST and ALT levels.

3.4. Expression of AT1R in the liver and HepG2 cells

To further explore the protective effect of AT1R blockade in hepatic steatosis observed in animal model, we performed *in vitro* studies using HepG2 cells. We first ascertained AT1R expression in HepG2 cells comparing

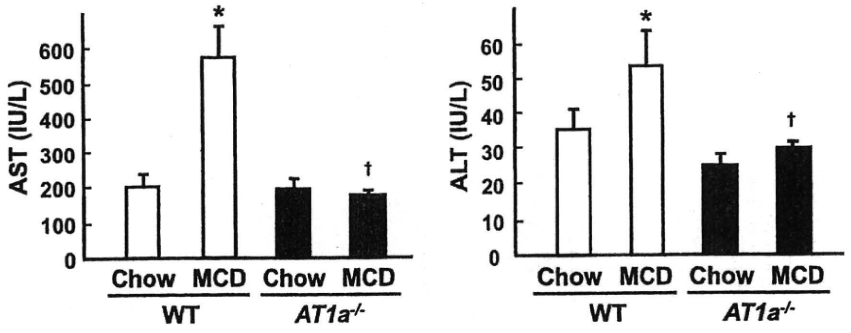

Fig. 2. Diminished hepatic injury following 8 weeks of MCD diet in the absence of AT1aR. AST and ALT levels were determined in WT (open bars) and $AT1a^{-/-}$ (closed bars) mice fed either normal chow or MCD diet for 8 weeks (n = 6/each group). $^{*}p < 0.05$, chow-fed vs. MCD diet-fed mice. $^{\dagger}p < 0.05$, WT vs. $AT1a^{-/-}$ mice.

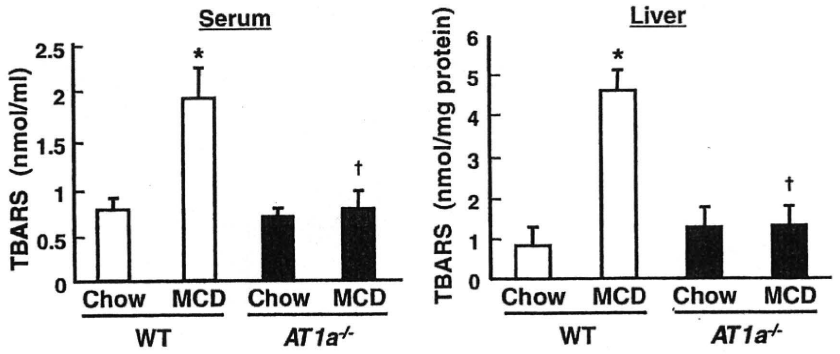

Fig. 3. Influence of AT1aR expression on TBARS levels in serum and liver. TBARS levels were assayed in serum (left panel) and liver (right panel) from WT (open bars) and $AT1a^{-/-}$ (closed bars) mice after feeding either normal chow or MCD diet (n = 6/each group). $^{*}p < 0.05$, chow-fed vs. MCD diet-fed mice. $^{\dagger}p < 0.05$, WT vs. $AT1a^{-/-}$ mice.

that of heart, kidney, and liver tissues, which are known to express functional AT1R. As displayed in Fig. 4, Western blot analysis revealed AT1R protein expression in HepG2 cells, supporting the previous *in vivo* binding assay of Ang II that detected a homogeneous signal pattern throughout the liver parenchyma [27]. Although the quantities of loaded protein were the same among samples, the band intensity in HepG2 appeared to be weaker compared to whole liver homogenate, which comprises non-parenchymal liver cells such as hepatic stellate cells and Kupffer cells. However, real-time PCR demonstrated similar level of AT1R in HepG2 as compared to kidney (Fig. 4, right panel).

3.5. *AT1R blockade reduces lipid accumulation in hepatocellular in vitro model*

To examine whether AT1R expression in HepG2 was functional, we utilized *in vitro* model of steatosis in which HepG2 cells were treated with FFAs mixture with or without 10 μM of telmisartan. As shown in Fig. 5A, Nile Red assay quantified 4- to 5-fold increase in cellular

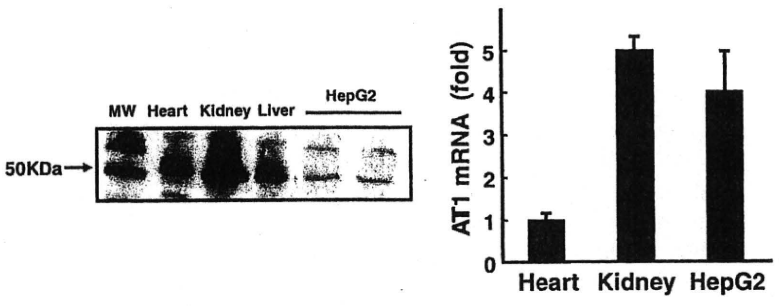

Fig. 4. Expressions of AT1R in the liver and HepG2 cells. Western blots of AT1R protein expression in homogenates from human liver and HepG2 cells by comparison with heart and kidney as positive tissues for AT1R expression (50 KDa) (left panel). Quantitative real-time PCR analysis for AT1R in HepG2 (right panel). Results represent from at least three independent experiments.

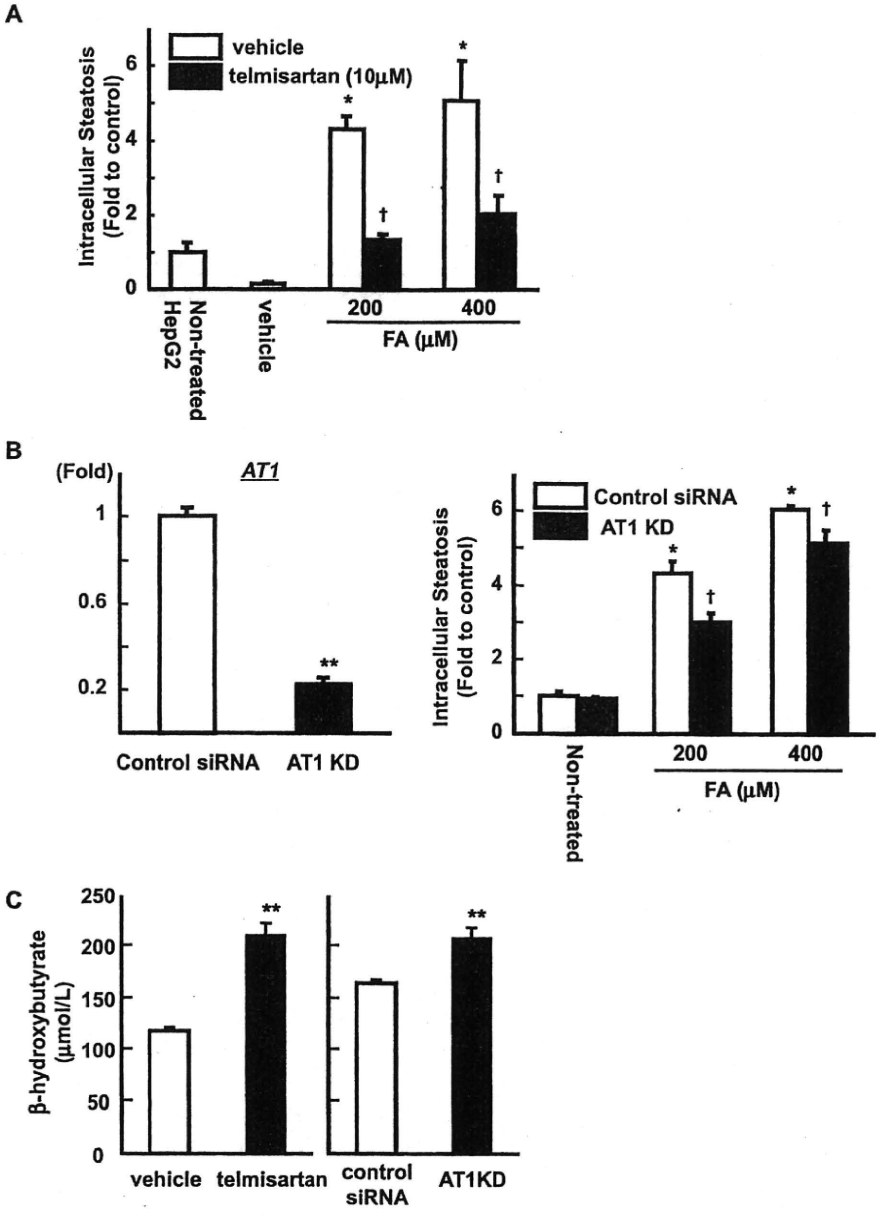

Fig. 5. AT1R blockade attenuates cellular steatosis following fatty acids overload. (A) Influence of telmisartan on intracellular steatosis induced by free fatty acids (FFAs) overload (2:1 oleate: palmitate) (n = 6/each group). (B) Effect of siRNA targeting AT1R on *AT1* mRNA expression (left panel) and influence of AT1 knockdown (KD) on cellular steatosis induced by FFAs overload (2:1 oleate: palmitate, right panel) (n = 6/each group). (C) Influence of AT1R blockade on β-hydroxybutyrate levels in media (n = 6/each group). $^{**}p < 0.005$, vs. control siRNA. $^{*}p < 0.05$, vs. non-treated groups. $^{\dagger}p < 0.05$, AT1R blockade (either by telmisartan or AT1 knockdown) vs. control (either vehicle or control siRNA) HepG2.

lipid accumulation when cells were treated with FFAs for 24 h in the absence of telmisartan. These changes were markedly attenuated by the presence of telmisartan by 60–70%. To exclude the possibility that these anti-steatotic effects might be attributable to pharmacological property of telmisartan, we investigated the influence of AT1R knockdown using siRNA in the same experimental model. As shown in Fig. 5B, transfection of HepG2 cells with siRNA targeting AT1R successfully depleted its mRNA expression by 80% when compared to control siRNA. This siRNA knockdown of AT1R resulted in significant 15–30% decrease in cellular lipid deposition following FFAs exposure (Fig. 5B, right panel). Compared to the treatment of telmisartan, the influence of AT1R knockdown appeared modest. This might be because siRNA suppression of AT1R was not sufficient to elicit complete inhibition of the AT1R signaling pathway. In connection with the observed ketogenesis in *AT1a*$^{-/-}$ mice, we examined β-hydroxybutyrate levels in the culture media. Under the condition

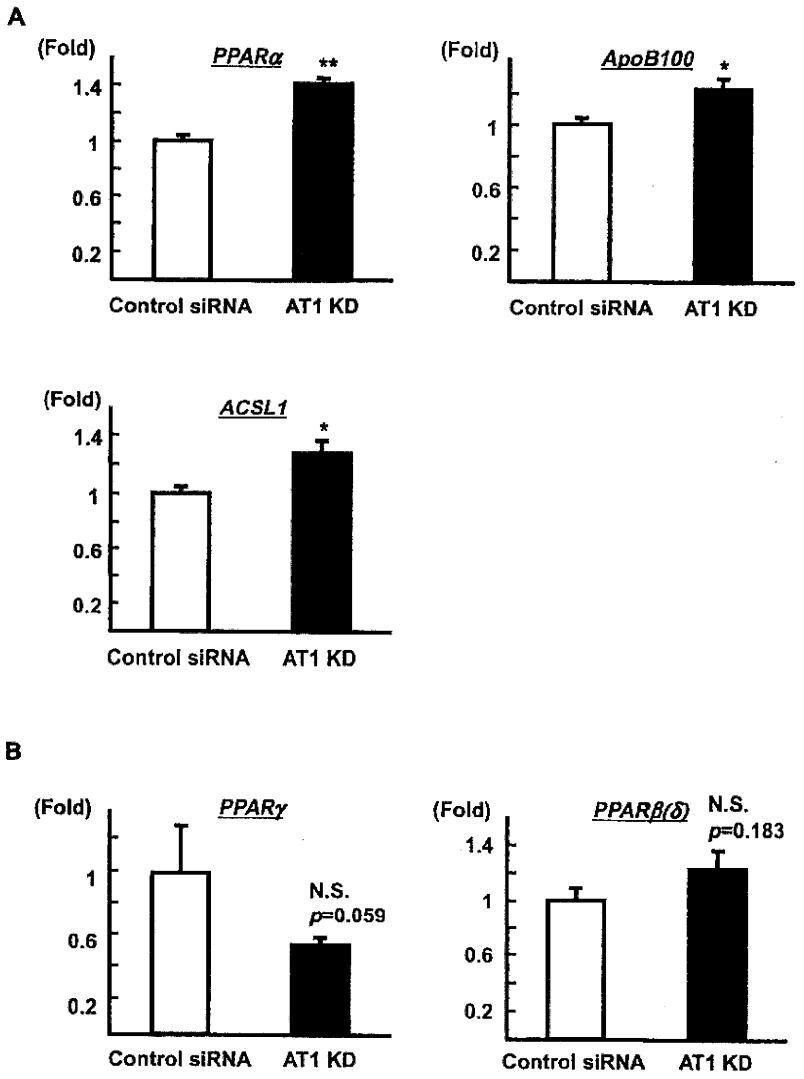

Fig. 6. Influence of AT1R knockdown on the expression of PPARα target genes (A) and the other PPAR isoforms (B). Real-time PCR quantified the expression of genes regulated by PPARα as well as of the other PPAR isoforms, PPARγ and PPARβ(δ) in HepG2 cells transfected with either siRNA targeting AT1R ($n = 6$) or negative control siRNA ($n = 6$). $^{*}p < 0.05$, vs. control siRNA. $^{**}p < 0.005$, vs. control siRNA. NS, not statistically significant.

of 200 μM of FFAs overload, the treatment of telmisartan as well as AT1R knockdown significantly increased β-hydroxybutyrate levels (Fig. 5C).

3.6. AT1R knockdown induces PPARa and its target genes

The observation that hepatic PPARα expression was up-regulated in *AT1a*$^{-/-}$ mice suggests the possible link between AT1R signaling and PPARα expression. In this setting, our working hypothesis was that AT1R down-regulation might in turn influence the hepatocellular expressions of PPARα and its target genes. As shown in Fig. 6A, transient AT1R silencing by siRNA resulted in significant up-regulation of *PPARα* by 41%. In addition, PPARα target genes, acyl-CoA synthetase 1 (*ACSL1*) and apolipoprotein B (*ApoB*) 100 were also induced by 27% and 21%, respectively. These data exclude the possibility that PPARα up-regulation in *AT1a*$^{-/-}$ mice might be resulted from chronic adaptation to the absence of AT1R. To exclude the possible contribution of the other PPAR isoforms in hepatocellular steatosis, the expression of PPARγ and PPARβ(δ) were assessed by real-time PCR, which resulted in no significant changes following AT1R depletion (Fig. 6B).

4. Discussion

The present study indicates a major role for AT1R in hepatic steatosis by providing a precise genetic approach. Homozygous disruption of AT1R in mice resulted in marked reduction of hepatic lipid accumulation as determined morphologically and by hepatic TG

content. Recent studies have demonstrated that ARBs improve insulin resistance and hyperinsulinemia. Because the improvement of insulin resistance leads to reduction of FFAs flux to the liver together with increased uptake and storage of FFAs in adipose tissue, ARBs are expected to reduce hepatic steatosis. However, the effect of ARBs on hepatic steatosis is still controversial [7,14,17,28–30]. These conflicting findings might be explained by differences in selective PPARγ modulating properties of ARBs [15,16], or attributed to differences in the dose and length of ARBs supplementation as well as potential differences in the mechanisms of steatosis in the different experimental models. Our data reinforces the theory that blockade of AT1R, unrelated to pharmacological properties of ARBs, ameliorates the development of hepatic steatosis.

The pathophysiology of NASH remains poorly understood, but is often described as "two-hit process" consisting of hepatic TG accumulation (the 1st step) and development of oxidative stress and proinflammatory cytokines (the 2nd step), which leads to hepatocyte injury, inflammation, and fibrosis [26]. Previous reports have demonstrated that pharmacological blockade or gene deletion of renin-angiotensin system (RAS) significantly attenuates hepatic fibrosis in experimental animal models [31,32]. Moreover, Ang II, the effecter peptide for AT1R, has been reported to stimulates an array of fibrogenic actions in activated HSCs through the mediation of reactive oxygen species [33]. More recent data has revealed that angiotensin converting enzyme (ACE) deficient ($ACE^{-/-}$) mice which exhibit reduced levels of Ang II by 70% in plasma and by 85–97% in tissues [34] showed pronounced increase in hepatic gene expression related to lipolysis and fatty acid oxidation, suggesting close link between RAS and hepatic lipid metabolism [35]. Taken together with our finding of the anti-steatotic effect, the blockade of AT1R appears to contribute to wide range of steps and phases in the pathogenesis of NASH.

The up-regulation of PPARα in the liver of $AT1a^{-/-}$ mice is intriguing because PPARα plays a central role in hepatic lipid homeostasis. It is well known that many of the genes encoding enzymes involved in the mitochondrial and peroxisomal fatty acid β-oxidation pathways are regulated by PPARα. To exclude the possibility that adaptation to persistent AT1R absence may induce PPARα expression in mice, we performed *in vitro* siRNA experiments, which confirmed induction of PPARα and its target genes by transient AT1R knockdown. In support of these observations, previous experiments have demonstrated telmisartan-mediated induction of PPARα [36]. Whereas induction of PPARα was observed in $AT1a^{-/-}$ mice, the present study lacks the direct evidence that suppressive effect of AT1R blockade on hepatic steatosis is mediated by PPARα. In this connection, we examined β-hydroxybutyrate levels since it is documented that PPARα activation leads to stimulation of ketogenesis [37,38]. This yielded marked increase in serum β-hydroxybutyrate in $AT1a^{-/-}$ mice. In addition, our *in vitro* experiments demonstrated significant increase in β-hydroxybutyrate in the culture media in response to AT1R blockade. These findings support the detected changes in gene expressions of PPARα and ACSL1 following AT1R deletion. Although it remains controversial whether the blockade of AT1R directly stimulates PPARα, up-regulation of PPARα likely increases the sensitivity to agonist and thus clinical usage of ARBs together with PPARα ligand such as fibrates might have synergistic effects on hepatic lipid metabolism.

A potential limitation of the present study is the use of MCD dietary animal model. Although this model develops steatohepatitis morphologically similar to human NASH with an increase in oxidative stress and has been widely used for the study of NASH, absence of insulin resistance has been reported [24,25,39,40]. Since insulin resistance is considered to be pivotal in the development of NASH, this model might not entirely reflect the natural course and the etiological background of human NASH [41,42]. Some other potential dietary models include *ad libitum* feeding of the high fat diet, which develops obesity and insulin resistance but not noticeable steatohepatitis [43]. Additionally, intragastric overfeeding of high fat diet induces NASH pathology, but some of the biological changes observed in the liver did not mimic human NASH [44]. Altogether, the study of pathophysiological process of NASH is limited by the lack of suitable experimental animal models [45]. Interestingly, the effect of olmesartan has been investigated in a genetically diabetic rat fed MCD diet [30]. In contrast to our findings, olmesartan reduced hepatic steatosis only in diabetic but not in control rats. In the present study, MCD diet caused increase in hepatic TG content associated with decrease in serum TG level, suggesting that impaired TG secretion from liver might contribute to hepatic steatosis. These changes were blunted in the absence of AT1R, implying improvement of TG secretion in $AT1a^{-/-}$ mice. This might be in part explained by the observation of *in vitro* experiment that AT1 knockdown induced ApoB which is requisite for the formation of very low density lipoprotein (VLDL).

In the present study, human hepatoma cell line HepG2 instead of rodent primary hepatocytes was utilized for *in vitro* model of cellular steatosis. This was based on the previous report that human primary hepatocytes and HepG2 cells reached similar levels of intracellular lipid accumulation close to that determined in hepatocytes from human steatosis liver [23]. In addition, the observed up-regulation of hepatic PPARα in $AT1a^{-/-}$ mice led to the speculation that PPARα might play a role in the anti-steatotic effect of AT1 blockade.

Because hepatic expression of PPARα and the sensitivity to it notably differ among species [46], human-derived cell line was applied.

In conclusion, mice lacking AT1R are resistant to the development of hepatic steatosis with up-regulation of PPARα in MCD diet-induced steatohepatitis model. Accordingly, the levels of TBARS, a marker of oxidative stress, as well as aminotransferases, indicators of liver damage were significantly attenuated in $AT1a^{-/-}$ mice. In addition, an *in vitro* experiment of hepatocellular steatosis revealed that blockade of AT1R by telmisartan and specific siRNA knockdown markedly decreased cellular lipid accumulation. Up-regulation of PPARα was also confirmed by transient AT1R knockdown. These data provide strong evidence that, in addition to pharmacological effect of ARBs on PPARγ activation, AT1R signaling is involved in hepatic lipid metabolism.

Acknowledgements

The authors thank Dr. Naseem Gaur for helpful discussion. This work was supported by a Grant-in-aid from the Ministry of Health, Labor and Welfare of Japan to S. Tazuma. This work was carried out in part at the Analysis Center of Life Science, Hiroshima University.

References

[1] Belfort R, Harrison SA, Brown K, Darland C, Finch J, Hardies J, et al. A placebo-controlled trial of pioglitazone in subjects with non-alcoholic steatohepatitis. N Engl J Med 2006;355:2297–2307.
[2] Promrat K, Lutchman G, Uwaifo GI, Freedman RJ, Soza A, Heller T, et al. A pilot study of pioglitazone treatment for non-alcoholic steatohepatitis. Hepatology 2004;39:188–196.
[3] Marchesini G, Brizi M, Bianchi G, Tomassetti S, Zoli M, Melchionda N. Metformin in non-alcoholic steatohepatitis. Lancet 2001;358:893–894.
[4] Antonopoulos S, Mikros S, Mylonopoulou M, Kokkoris S, Giannoulis G. Rosuvastatin as a novel treatment of non-alcoholic fatty liver disease in hyperlipidemic patients. Atherosclerosis 2006;184:233–234.
[5] Basaranoglu M, Acbay O, Sonsuz A. A controlled trial of gemfibrozil in the treatment of patients with non-alcoholic steatohepatitis. J Hepatol 1999;31:384.
[6] Jin H, Yamamoto N, Uchida K, Terai S, Sakaida I. Telmisartan prevents hepatic fibrosis and enzyme-altered lesions in liver cirrhosis rat induced by a choline-deficient L-amino acid-defined diet. Biochem Biophys Res Commun 2007;364:801–807.
[7] Fujita K, Yoneda M, Wada K, Mawatari H, Takahashi H, Kirikoshi H, et al. Telmisartan, an angiotensin II type 1 receptor blocker, controls progress of non-alcoholic steatohepatitis in rats. Dig Dis Sci 2007;52:3455–3464.
[8] Bataller R, Gines P, Nicolas JM, Gorbig MN, Garcia-Ramallo E, Gasull X, et al. Angiotensin II induces contraction and proliferation of human hepatic stellate cells. Gastroenterology 2000;118:1149–1156.
[9] Kanno K, Tazuma S, Nishioka T, Hyogo H, Chayama K. Angiotensin II participates in hepatic inflammation and fibrosis through MCP-1 expression. Dig Dis Sci 2005;50:942–948.
[10] Yokohama S, Yoneda M, Haneda M, Okamoto S, Okada M, Aso K, et al. Therapeutic efficacy of an angiotensin II receptor antagonist in patients with non-alcoholic steatohepatitis. Hepatology 2004;40:1222–1225.
[11] Dahlof B, Devereux RB, Kjeldsen SE, Julius S, Beevers G, de Faire U, et al. Cardiovascular morbidity and mortality in the Losartan Intervention For Endpoint reduction in hypertension study (LIFE): a randomised trial against atenolol. Lancet 2002;359:995–1003.
[12] Henriksen EJ, Jacob S, Kinnick TR, Teachey MK, Krekler M. Selective angiotensin II receptor antagonism reduces insulin resistance in obese Zucker rats. Hypertension 2001;38:884–890.
[13] Sugimoto K, Kazdova L, Qi NR, Hyakukoku M, Kren V, Simakova M, et al. Telmisartan increases fatty acid oxidation in skeletal muscle through a peroxisome proliferator-activated receptor-gamma dependent pathway. J Hypertens 2008;26:1209–1215.
[14] Ibanez P, Solis N, Pizarro M, Aguayo G, Duarte I, Miquel JF, et al. Effect of losartan on early liver fibrosis development in a rat model of non-alcoholic steatohepatitis. J Gastroenterol Hepatol 2007;22:846–851.
[15] Benson SC, Pershadsingh HA, Ho CI, Chittiboyina A, Desai P, Pravenec M, et al. Identification of telmisartan as a unique angiotensin II receptor antagonist with selective PPARgamma-modulating activity. Hypertension 2004;43:993–1002.
[16] Schupp M, Janke J, Clasen R, Unger T, Kintscher U. Angiotensin type 1 receptor blockers induce peroxisome proliferator-activated receptor-gamma activity. Circulation 2004;109:2054–2057.
[17] Hirose A, Ono M, Saibara T, Nozaki Y, Masuda K, Yoshioka A, et al. Angiotensin II type 1 receptor blocker inhibits fibrosis in rat non-alcoholic steatohepatitis. Hepatology 2007;45:1375–1381.
[18] Burson JM, Aguilera G, Gross KW, Sigmund CD. Differential expression of angiotensin receptor 1A and 1B in mouse. Am J Physiol 1994;267:E260–E267.
[19] Sugaya T, Nishimatsu S, Tanimoto K, Takimoto E, Yamagishi T, Imamura K, et al. Angiotensin II type 1a receptor-deficient mice with hypotension and hyperreninemia. J Biol Chem 1995;270:18719–18722.
[20] Bligh EG, Dyer WJ. A rapid method of total lipid extraction and purification. Can J Biochem Physiol 1959;37:911–917.
[21] Malhi H, Bronk SF, Werneburg NW, Gores GJ. Free fatty acids induce JNK-dependent hepatocyte lipoapoptosis. J Biol Chem 2006;281:12093–12101.
[22] Greenspan P, Fowler SD. Spectrofluorometric studies of the lipid probe, nile red. J Lipid Res 1985;26:781–789.
[23] Gomez-Lechon MJ, Donato MT, Martinez-Romero A, Jimenez N, Castell JV, O'Connor JE. A human hepatocellular in vitro model to investigate steatosis. Chem Biol Interact 2007;165:106–116.
[24] Tomita K, Oike Y, Teratani T, Taguchi T, Noguchi M, Suzuki T, et al. Hepatic AdipoR2 signaling plays a protective role against progression of non-alcoholic steatohepatitis in mice. Hepatology 2008;48:458–473.
[25] Igolnikov AC, Green RM. Mice heterozygous for the Mdr2 gene demonstrate decreased PEMT activity and diminished steatohepatitis on the MCD diet. J Hepatol 2006;44:586–592.
[26] Day CP, James OF. Steatohepatitis: a tale of two "hits? Gastroenterology 1998;114:842–845.
[27] Paizis G, Cooper ME, Schembri JM, Tikellis C, Burrell LM, Angus PW. Up-regulation of components of the renin-angiotensin system in the bile duct-ligated rat liver. Gastroenterology 2002;123:1667–1676.
[28] Ran J, Hirano T, Adachi M. Angiotensin II infusion increases hepatic triglyceride production via its type 2 receptor in rats. J Hypertens 2005;23:1525–1530.
[29] Sugimoto K, Qi NR, Kazdova L, Pravenec M, Ogihara T, Kurtz TW. Telmisartan but not valsartan increases caloric expenditure

and protects against weight gain and hepatic steatosis. Hypertension 2006;47:1003–1009.
[30] Kurita S, Takamura T, Ota T, Matsuzawa-Nagata N, Kita Y, Uno M, et al. Olmesartan ameliorates a dietary rat model of non-alcoholic steatohepatitis through its pleiotropic effects. Eur J Pharmacol 2008;588:316–324.
[31] Yoshiji H, Kuriyama S, Yoshii J, Ikenaka Y, Noguchi R, Nakatani T, et al. Angiotensin-II type 1 receptor interaction is a major regulator for liver fibrosis development in rats. Hepatology 2001;34:745–750.
[32] Kanno K, Tazuma S, Chayama K. AT1A-deficient mice show less severe progression of liver fibrosis induced by CCl(4). Biochem Biophys Res Commun 2003;308:177–183.
[33] Bataller R, Schwabe RF, Choi YH, Yang L, Paik YH, Lindquist J, et al. NADPH oxidase signal transduces angiotensin II in hepatic stellate cells and is critical in hepatic fibrosis. J Clin Invest 2003;112:1383–1394.
[34] Campbell DJ, Alexiou T, Xiao HD, Fuchs S, McKinley MJ, Corvol P, et al. Effect of reduced angiotensin-converting enzyme gene expression and angiotensin-converting enzyme inhibition on angiotensin and bradykinin peptide levels in mice. Hypertension 2004;43:854–859.
[35] Jayasooriya AP, Mathai ML, Walker LL, Begg DP, Denton DA, Cameron-Smith D, et al. Mice lacking angiotensin-converting enzyme have increased energy expenditure, with reduced fat mass and improved glucose clearance. Proc Natl Acad Sci USA 2008;105:6531–6536.
[36] Clemenz M, Frost N, Schupp M, Caron S, Foryst-Ludwig A, Bohm C, et al. Liver-specific peroxisome proliferator-activated receptor alpha target gene regulation by the angiotensin type 1 receptor blocker telmisartan. Diabetes 2008;57:1405–1413.
[37] Mandard S, Müller M, Kersten S. Peroxisome proliferator-activated receptor alpha target genes. Cell Mol Life Sci 2004;61:393–416.
[38] Luci S, Giemsa B, Kluge H, Eder K. Clofibrate causes an upregulation of PPAR-{alpha} target genes but does not alter expression of SREBP target genes in liver and adipose tissue of pigs. Am J Physiol Regul Integr Comp Physiol 2007;293:R70–R77.
[39] Rinella ME, Green RM. The methionine–choline deficient dietary model of steatohepatitis does not exhibit insulin resistance. J Hepatol 2004;40:47–51.
[40] Vetelainen R, van Vliet A, van Gulik TM. Essential pathogenic and metabolic differences in steatosis induced by choline or methione-choline deficient diets in a rat model. J Gastroenterol Hepatol 2007;22:1526–1533.
[41] Pagano G, Pacini G, Musso G, Gambino R, Mecca F, Depetris N, et al. Non-alcoholic steatohepatitis, insulin resistance, and metabolic syndrome: further evidence for an etiologic association. Hepatology 2002;35:367–372.
[42] Sanyal AJ, Campbell-Sargent C, Mirshahi F, Rizzo WB, Contos MJ, Sterling RK, et al. Nonalcoholic steatohepatitis: association of insulin resistance and mitochondrial abnormalities. Gastroenterology 2001;120:1183–1192.
[43] Collins S, Martin TL, Surwit RS, Robidoux J. Genetic vulnerability to diet-induced obesity in the C57BL/6J mouse: physiological and molecular characteristics. Physiol Behav 2004;81:243–248.
[44] Deng QG, She H, Cheng JH, French SW, Koop DR, Xiong S, et al. Steatohepatitis induced by intragastric overfeeding in mice. Hepatology 2005;42:905–914.
[45] Koteish A, Mae Diehl A. Animal models of steatohepatitis. Best Pract Res Clin Gastroenterol 2002;16:679–690.
[46] Gonzalez FJ, Peters JM, Cattley RC. Mechanism of action of the nongenotoxic peroxisome proliferators: role of the peroxisome proliferator-activator receptor alpha. J Natl Cancer Inst 1998;90:1702–1709.

GASTROENTEROLOGY 2009;137:673–681

Amphipathic DNA Polymers Inhibit Hepatitis C Virus Infection by Blocking Viral Entry

TAKUYA MATSUMURA,* ZONGYI HU,* TAKANOBU KATO,* MARLENE DREUX,‡ YONG-YUAN ZHANG,* MICHIO IMAMURA,§ NOBUHIKO HIRAGA,§ JEAN-MARC JUTEAU,‖ FRANCOIS-LOIC COSSET,‡ KAZUAKI CHAYAMA,§ ANDREW VAILLANT,‖ and T. JAKE LIANG*

*Liver Diseases Branch, National Institute of Diabetes and Digestive and Kidney Diseases, National Institutes of Health, Bethesda, Maryland; ‡Universite de Lyon, INSERM U758, and Ecole Normale Superieure de Lyon, Lyon, France; §Department of Medicine and Molecular Science, Division of Frontier Medical Science, Graduate School of Biomedical Sciences, Hiroshima University, Hiroshima, Japan; and ‖REPLICor Inc, Laval, Quebec, Canada

See editorial on page 427.

BACKGROUND & AIMS: Hepatitis C virus (HCV) gains entry into susceptible cells by interacting with cell surface receptor(s). Viral entry is an attractive target for antiviral development because of the highly conserved mechanism. **METHODS:** HCV culture systems were used to study the effects of phosphorothioate oligonucleotides (PS-ONs), as amphipathic DNA polymers (APs), on HCV infection. The in vivo effects of APs were tested in urokinase plasminogen activator (uPA)/severe combined immunodeficient (SCID) mice engrafted with human hepatocytes. **RESULTS:** We show the sequence-independent inhibitory effects of APs on HCV infection. APs were shown to potently inhibit HCV infection at submicromolar concentrations. APs exhibited a size-dependent antiviral activity and were equally active against HCV pseudoparticles of various genotypes. Control phosphodiester oligonucleotide (PO-ON) polymer without the amphipathic structure was inactive. APs had no effect on viral replication in the HCV replicon system or binding of HCV to cells but inhibited viral internalization, indicating that the target of inhibition is at the postbinding, cell entry step. In uPA/SCID mice engrafted with human hepatocytes, APs efficiently blocked de novo HCV infection. **CONCLUSIONS: Our results demonstrate that APs are a novel class of antiviral compounds that hold promise as a drug to inhibit HCV entry.**

Hepatitis C virus (HCV) infects approximately 200 million people worldwide.[1] The majority of HCV-infected patients fails to clear the virus, and many develop chronic liver disease including cirrhosis with a risk of hepatocellular carcinoma. Treatment of chronic hepatitis C is currently based on peginterferon-alfa and ribavirin, which is accompanied by substantial adverse effects and is only effective in approximately half of the patients.[2,3] In addition to other viral targets, viral entry is an attractive target for antiviral development because of the potentially conserved mechanism of viral entry.[4] Although several candidate receptors for HCV have been identified,[5–10] the mechanism of HCV entry still remains largely unknown. Previous reports have indicated a pH dependency for entry of HCV pseudoparticles (HCVpp) as well as cell culture-generated HCV (HCVcc), suggesting that HCV enters cells by receptor-mediated endocytosis.[7,11,12] Antiviral compounds targeting the entry step of viral infection have been successfully developed in other viral infections.[13] Recent studies have shown that phosphorothioate oligonucleotides (PS-ONs), as amphipathic DNA polymers (APs), have a sequence-independent antiviral activity against human immunodeficiency virus type 1 (HIV-1) as entry inhibitors.[14] The antiviral effect of APs appears to be specific to the phosphorothioate backbone, which confers an amphipathic structure, because the phosphodiester oligonucleotides (PO-ONs) as nonamphipathic polymers are ineffective.[14]

Materials and Methods

Cell Culture and Oligonucleotide Synthesis

Huh7.5 (provided by Charles Rice), Huh7.5.1 (provided by Francis Chisari), Huh7, and Hep3B cells were maintained at 37°C, 5% CO_2 in Dulbecco's modified Eagle medium, containing 10% fetal bovine serum. All PS-ONs and PO-ONs were synthesized as described previously.[14] Oligonucleotides lacking the phosphorothioate modification (PO-ONs) were synthesized with the addition of 2′-O-methyl ribose modification, which stabilizes oligonucleotides from nuclease degradation.[14] Compounds used in the in vivo experiment were synthesized under good manufacturing practice (GMP) conditions to yield high-purity sodium salts.

Abbreviations used in this paper: APs, amphipathic DNA polymers; HCV, hepatitis C virus; HCVcc, cell culture-generated HCV; HCVpp, HCV pseudoparticles; VSVGpp, vesicular stomatitis virus G protein pseudoparticle; PO-ON, phosphodiester oligonucleotide; PS-ONs, phosphorothioate oligonucleotides.

0016-5085/09/$36.00
doi:10.1053/j.gastro.2009.04.048

HCV Infection and Replication Assays

The production of cell culture-generated HCV JFH-1 (HCVcc) and HCV pseudovirus (HCVpp) has been reported previously[5,15] and is described in detail in the Supporting Document. HCVpp harboring E1/E2 glycoproteins from genotypes 1a, 1b, 2a, 3a, 4a, 5a, and 6a were described previously.[16] For viral internalization assay, Hep3B cells were incubated for 1 hour at 4°C to allow binding of HCVpp (pHCV7a) to cells, washed repeatedly with phosphate-buffered saline to remove unbound virus, and treated with concanamycin A (Sigma-Aldrich, St. Louis, MO) (25 nmol/L), Anti-E2 AP33 antibody[17] (25 μg/mL), PS-ON (100 nmol/L), or PO-ON (100 nmol/L) overnight at 37°C for viral entry. The efficiency of infection was measured by luciferase assay 24 hours later. Transient assay of genotypes 1b (Con-1) and 2a (JFH-1) subgenomic reporter replicons have been reported previously[18,19] and are described in detail in the Supporting Document.

HCV Binding and Fusion Assays

The HCV-like particle (LP) binding assay was performed at 4°C for 1 hour in 100 μL of TNC (50 mmol/L Tris, pH 7.4, 100 mmol/L NaCl, 1 mmol/L $CaCl_2$) buffer containing 1% bovine serum albumin as reported previously[20] and is described in detail in the Supporting Document. Both Hep3B and Huh7.5 cells were tested. Direct binding of PS-ON or PO-ON to HCV-LP was measured by a plate-binding assay and is described in the Supporting Document. For viral fusion assay, HCVpp/liposome lipid mixing assays with rhodamine-labelled liposomes were performed as previously reported[21] and are described in the Supporting Document.

HCV Infection in Chimeric Mice

Human hepatocyte-transplanted mice generated in severe combined immunodeficient (SCID)/urokinase plasminogen activator (uPA) mice were purchased from PhenixBio (Hiroshima, Japan).[22] These uPA/SCID mice stably transplanted with human hepatocytes were treated intraperitoneally with 10 mg/kg of poly C PS-ON or poly AC PS-ON (40mer) on days −1, 0, 1, 3, 5, and 7. Control poly C PO-ON (40mer stabilized by 2′-O-methyl ribose modification) was also tested. A fourth group of mice did not receive any compounds (only normal saline administration). Approximately 5–15 mice were included in each group. The mice were intravenously inoculated on day 0 with HCV patient serum containing 3.9×10^3 copies of HCV genotype 1b. Serum samples were obtained on days 0 (prior to HCV inoculation), 7, 14, 21, 28, and 35 for HCV RNA, HCV core antigen, and human albumin determination. Human albumin in the blood of the chimeric mice was measured with the Alb-II Kit (Eiken Chemical, Tokyo, Japan).

Statistical Analysis

Data from at least triplicate experiments were averaged and expressed as means ± standard deviations. Statistical analysis was performed using the Student *t* test or Welch *t* test. *P* values of less than .05 were considered statistically significant.

Results

APs Inhibit HCV Infection in a Sequence-Independent Manner

To assess whether APs can inhibit HCV infection, fully degenerate 40mer oligonucleotides that were either phosphorothioated (PS-ON) resulting in a stable amphipathic DNA polymer or that had a 2′-O-methyl modification on the ribose moiety (PO-ON) conferring stability but not altering the polyanionic nature of DNA[14,23] were tested. Huh7.5 cells were infected with HCVcc in the presence of either PS-ON or PO-ON. At 72 hours postinfection, HCV-infected cells were assessed by immunofluorescence assay (Figure 1*A*) and intracellular HCV RNA quantification (Figure 1*B*). HCV infection was significantly inhibited by PS-ON and not PO-ON ($P < .05$). The inhibitory effect of PS-ON was also confirmed by reduced HCV core antigen and HCV RNA levels in the culture supernatant, as compared with those of the PO-ON-treated cells ($P < .05$) (Figure 1*C* and *D*). To evaluate further the efficacy of PS-ON against viral entry, HCVpp harboring genotype 1b was used to infect Hep3B. The PS-ON blocked infection of HCVpp in a similar dose-dependent manner (Figure 1*E*). The PO-ON exhibited some inhibitory effect at high concentration, which could be attributed to noncytotoxic inhibition of cellular adherence by the polyanion nature of PO-ON. To assess whether the PS-ON inhibitory effect is specific for HCV, retroviral pseudovirus carrying the vesicular stomatitis virus G protein (VSVGpp) was tested in the presence of PS-ON or PO-ON. Neither PS-ON nor PO-ON had any effect on VSVGpp infection (Figure 1*F*). Furthermore, adenoviral infection was not inhibited by PS-ON (Supplementary Figure 1).

A series of homo- and heteropolymeric APs including poly G, A, T, C, TG AC, TC, and AG PS-ONs were tested for their inhibitory activities on HCV infection in both HCVcc and the HCVpp systems. These APs had similar inhibitory activities as the degenerate PS-ON with random sequence in the HCVcc system except for poly G and poly A (Figure 2*A*). Similar effects were also observed on HCV core antigen and HCV RNA levels in the culture supernatant (Figure 2*B* and *C*). In the HCVpp system, these PS-ONs also had similar inhibitory effects (Figure 2*D*).

AP Inhibition of HCV Infection Is Dependent on Size and Amphipathicity

Different sizes of degenerate PS-ONs (6-, 10-, 20-, 30-, 40-, 50- and 80mer) were tested for their inhibitory

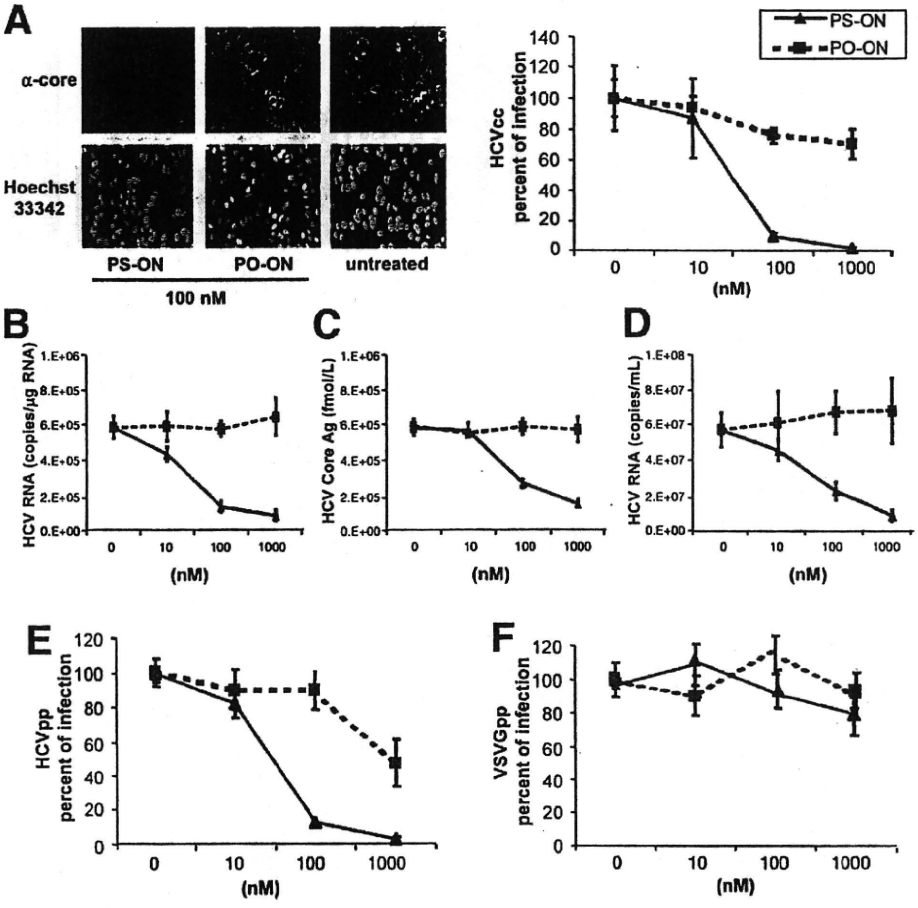

Figure 1. Effect of PS-ON on HCV infection. (*A*) Huh7.5 cells were infected with HCVcc in the presence of various concentrations of 40mer PS-ON or PO-ON (degenerate sequence). Two days after infection, infected cells were detected by immunofluorescence assay using anticore antibodies (*left panel*). Percentage of infection was determined by dividing the number of HCV-expressing cells in treated over the untreated cells (*right panel*). The intracellular HCV RNA levels (*B*) and HCV core Ag (*C*) and supernatant HCV RNA (*D*) levels in the culture medium were determined. Hep3B cells were infected with (*E*) HCVpp genotype 1b or (*F*) VSVGpp and treated with various concentrations of PS-ON and PO-ON, and luciferase activities were determined 2 days later. Results are shown as percentages of infection + standard deviations (SD).

activities in the HCVcc and HCVpp systems. Only PS-ONs with lengths of 40mer or greater potently inhibited HCV infection (Figure 2*E*). This result was confirmed with the poly C PS-ONs (Supplementary Figure 2). To determine the requirement of amphipathicity for antiviral activity of these compounds, additional oligonucleotide analogs that had diminished hydrophilic character were prepared and include degenerate PS-ON analogs with either the base and/or the sugar removed (Supplementary Figure 3). An additional degenerate PS-ON analog containing the 2′-O-methyl ribose modification that does not affect the amphipathicity was tested. These analogs were tested for their inhibitory activities in the HCVcc and HCVpp systems. Only analogs that retained the amphipathic properties inhibited HCV infection (Figure 2*F*). These observations suggest that the amphipathic nature of these PS-ONs is necessary for inhibiting HCV infection.

APs Inhibit Infection of Various Genotypes of HCV Without Affecting Replication and Cell Attachment

To study the effects of APs on various HCV genotypes, HCVpp harboring E1/E2 glycoproteins from genotypes 1a, 1b, 2a, 3a, 4a, 5a, and 6a were tested.[16] Infections by all genotypes were equally blocked by the degenerate PS-ON, whereas the degenerate PO-ON had no effect (Figure 3*A*). Similar observation was obtained with the poly C compounds (Supplementary Figure 2*D*).

The degenerate PS-ON compound was tested for its effect on viral replication in the HCV replicon system, which supports viral replication without the viral entry step. Genotype 1b and 2a subgenomic replicons were tested. Subgenomic replicon RNAs containing luciferase reporter were transfected into Huh7.5 cells, and the replication efficiency was determined in the presence of the PS-ON or PO-ON control. Neither PS-ON nor PO-ON displayed any antiviral activities in both subgenomic replicon systems (Figure 3*B*). To eliminate the possibility that PS-ON may induce an antiviral state with increasing time of exposure to cells, the HCV replicon assay was performed after exposure to either PS-ON or PO-ON for 24–48 hours, and no difference in replication was observed (data not shown). Furthermore, Huh7.5 cells treated with PS-ON or PO-ON did not produce any detectable levels of type I interferons.

To dissect further the effect of PS-ON on viral entry, we applied the HCV-LP binding assay, which has been

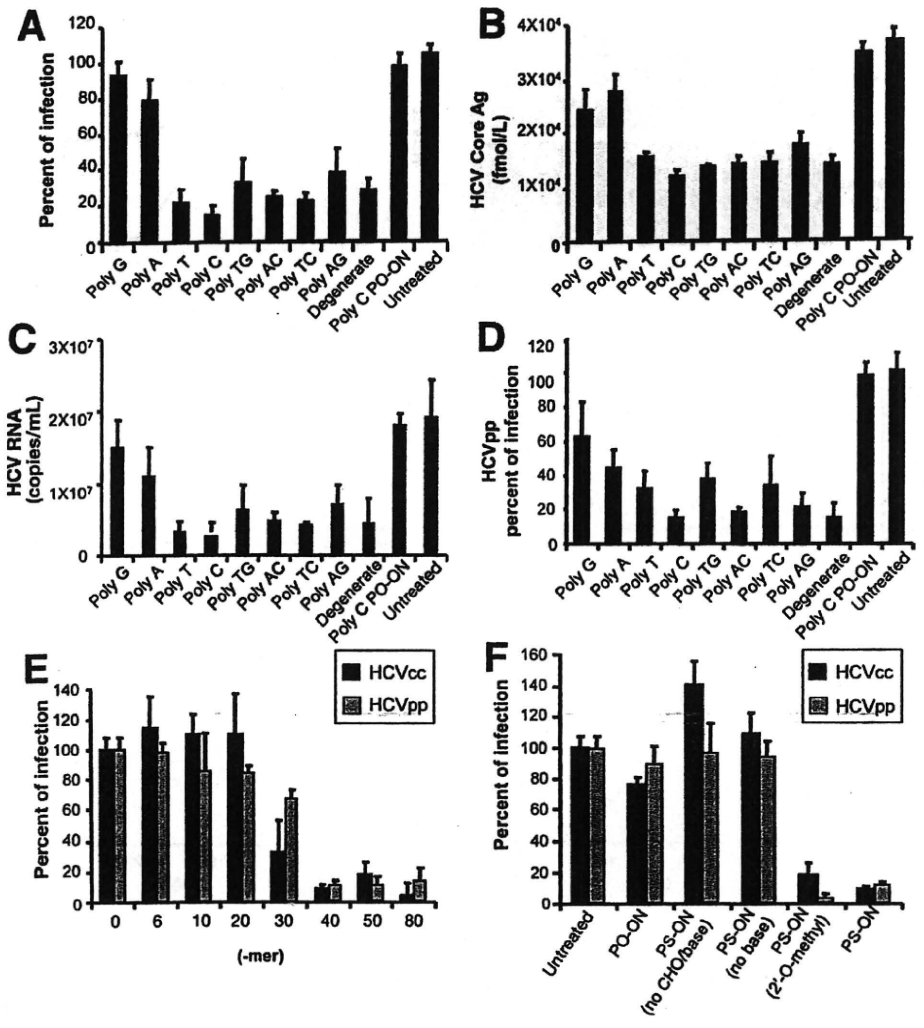

Figure 2. Sequence-independent and size- and phosphorothioation-dependent effects of PS-ON on HCV infection. A series of 40mer PS-ONs with specific sequences including poly poly G, A, T, C, TG AC, TC, and AG were tested for their inhibitory effect on HCV infection. (*A*) HCVcc was inoculated with Huh7.5 cells and treated with 100 nmol/L of these homo- and heteropolymeric PS-ONs. Expression of HCV core was detected by immunofluorescence assay using anticore antibodies. (*B*) The HCV core Ag titers and (*C*) HCV RNA levels in the culture medium were determined. (*D*) Hep3B cells were infected with HCVpp genotype 1b and treated with these various PS-ONs at 100 nmol/L, and luciferase activities were determined 2 days later. (*E*) Various sizes of PS-ON (10–80mers) at 100 nmol/L were tested in the HCVcc and HCVpp systems. (*F*) Various structures of oligonucleotides, PS-ON analogue with phosphorothioate backbone but without the sugar or base, and PS-ON analogue with 2′-O-methyl ribose modification, were synthesized. Each 40mer oligonucleotide at 100 nmol/L was tested in the HCVcc and HCVpp systems. All results are shown as percentages of infection + SD.

developed as a surrogate system to assess HCV binding to cells.[24–26] HCV-LP were incubated in the presence of PS-ON and PO-ON for 1 hour at 4°C with Huh7.5 or Hep3B cells. Under this condition, virus attaches to the cells but does not enter. HCV patients' serum containing high-level of anti-E1/E2 antibodies was included as a control. The binding was detected with FITC-labeled mouse monoclonal anti-E2 antibodies (Figure 3*C*). The results showed that the anti-HCV antibodies inhibited the HCV-LP binding to the cells, whereas the PS-ON and PO-ON-treated HCV-LP did not inhibit HCV-LP binding. To validate the HCV-LP binding assay, HCVcc binding to cells was performed in the presence of PS-ON, PO-ON, or HCV serum. HCV RNA bound to the cells was quantified to determine the percentage of binding. As shown in Figure 3*D*, HCV antibody significantly inhibited HCVcc binding to cells (~80%), whereas PS-ON and PO-ON had minor effects (<20%). These results suggest that the target of inhibition by APs is at the postbinding, cell entry step.

To address the question of whether PS-ON binds to HCV directly to inhibit HCV infection, HCV binding assays were performed. First, in an immunoassay format using HCV-LP as a capture antigen, neither PS-ON nor PO-ON showed any significant binding to HCV-LP (Table 1). Second, sedimentation density gradient analysis did not show a preferential cosedimentation of HCVcc with PS-ON or PO-ON in comparison with the control preparation (Figure 3*E*), indicating that neither PS-ON nor PO-ON binds to HCVcc to any significant extent. The amount of PS-ON in the HCVcc or the control fraction was higher than that of PO-ON, probably reflecting the different physical properties of PS-ON and PO-ON. However, it is possible that low-affinity binding of HCV and PS-ON could be present and required for subsequent inhibitory action but not detected by the currently applied assays.

APs Inhibit Viral Internalization

To determine which entry step that APs targets, the HCVpp assay was performed in the presence of concanamycin A (25 nmol/L), degenerate PS-ON (100 nmol/L), degenerate PO-ON (100 nmol/L), or AP33+ALP98

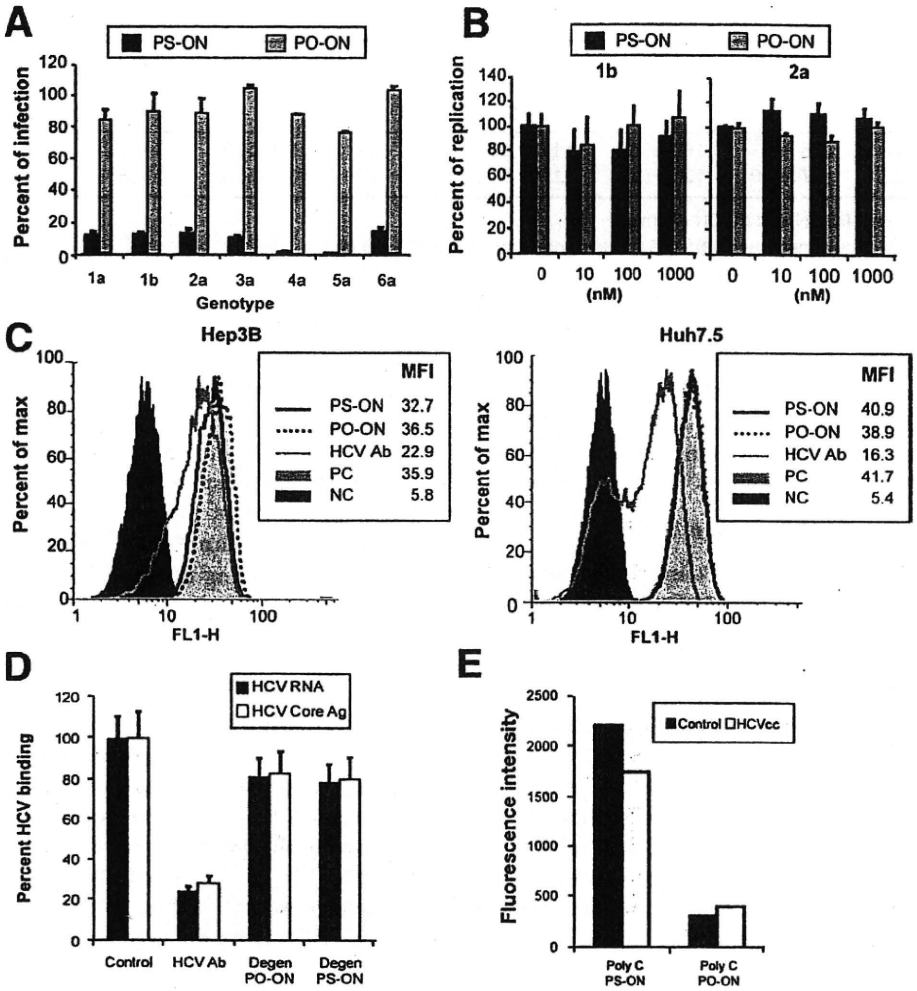

Figure 3. Effects of PS-ON on infection of various HCV genotypes, HCV replication, and cell binding. (*A*) HCVpp harboring E1/E2 glycoproteins from genotypes 1a, 1b, 2a, 3a, 4a, 5a, and 6a were inoculated into Hep3B cells and simultaneously treated with 100 nmol/L of degenerate PS-ON and PO-ON (40mer). Luciferase activities were determined 2 days later. (*B*) Subgenomic RNA of genotype 1b Con1 or 2a JFH1 were transfected into Huh7.5 cells. Four hours after transfection, a set of transfected cells was harvested as a control for transfection efficacy, and the remaining cells were treated with 100 nmol/L of PS-ON and PO-ON. Cells were then harvested at 72 hours posttransfection and luciferase activities determined. The replication level was presented as the ratio of the luciferase activity of the sample at 72 hours over that of 4 hours. Percentages of replication were determined by dividing the replication level of treated over that of untreated samples. (*C*) Hep3B and Huh7.5 cells were incubated with 20 μg/mL HCV-LP and 100 nmol/L PS-ON or PO-ON at 4°C for 1 hour. The cells were washed and incubated with anti-E2 ALP98 monoclonal antibody for 30 minutes followed by FITC-labeled goat anti-mouse immunoglobulin for 30 minutes at 4°C. HCV-LP binding was analyzed by flow cytometry. The *black filled peaks* are negative controls without the anti-E2 antibody. The *gray filled peaks* are positive controls showing HCV-LP binding without any compounds. The *black solid lines* and *gray dotted lines* represent treatments with PS-ON and PO-ON, respectively. The *gray solid line* represents samples in the presence of HCV serum that has been shown previously to inhibit HCV-LP binding. The mean fluorescence intensity (*MFI*) of each sample is shown. (*D*) HCVcc was incubated with Huh7.5 cells in the presence of HCV serum PS-ON or PO-ON at 4°C for 1 hour. The unbound virus was washed off, and the bound HCVcc was determined by HCV RNA quantification and HCV core Ag assay. (*E*) HCVcc was incubated with Cy3-labeled degenerate PS-ON or PO-ON (40mer) and subjected to iodixinol density gradient analysis as described in the online Supporting Document. Control preparation generated the same way was used for comparison. The fluorescence intensity of the fraction where infectious HCV sedimented was determined and shown.

monoclonal anti-E2 antibodies (25 μg/mL total concentration) at 37°C. Hep3B cells were first incubated with HCVpp at 4°C to allow binding and then at 37°C with various compounds after the inoculating HCVpp was removed. Concanamycin A is known to inhibit HCV entry by preventing acidification of endosome.[12] As shown in Figure 4*A*, AP33+ALP98 anti-E2 antibodies blocked HCV binding to the cells but had no effect on HCV entry. On the other hand, both concanamycin A and the degenerate PS-ON inhibited HCV entry.

To demonstrate that APs may inhibit HCV internalization at the fusion step, a viral fusion assay was performed with HCVpp or VSVpp as control.[21] Degenerate sequence and poly C PS-ONs and the control PO-ONs

Table 1. Lack of Binding of PS-ON to HCV-LP

	PS-ON (nmol/L)[a]				PO-ON (nmol/L)[a]				AP33[b]
	0	10	100	1000	0	10	100	1000	1 μg/mL
HCV-LP	155 + 14	105 + 9	162 + 13	116 + 10	137 + 12	15 + 10	123 + 12	157 + 13	1475 + 150
Control	147 + 13	117 + 10	120 + 11	117 + 9	111 + 10	33 + 14	100 + 8	103 + 9	153 + 16

[a]Cy3 labeled degenerate PS-ON and PO-ON (40mer).
[b]AP33 binding to HCV-LP was detected with Cy3-labeled goat anti-mouse IgG antibody.

were tested. Both PS-ON compounds showed significant inhibition of HCVpp fusion over their control PO-ON, whereas VSVGpp fusion was largely unaffected by either PS-ON or PO-ON (Figure 4*B* and Supplementary Figure 4). The inhibitory effect of PS-ON on fusion was evident on both the rate and maximum of fusion in the assay.

APs Inhibit HCV Infection In Vivo

To test the efficiency of APs in vivo, sodium salts of amphipathic polymers (40mers) of poly C and poly AC and their respective PO-ON controls were prepared. Degenerate oligonucleotides were avoided because they might potentially contain CpG motifs, which could induce endogenous interferons, although in vitro testing did not reveal such a possibility. Human hepatocyte-transplanted uPA/SCID mice were treated with these compounds as described and inoculated with infectious HCV genotype 1b patient serum. In this model, the production of human albumin in serum was monitored for the engraftment index of human hepatocytes. All mice showed robust and comparable human albumin concentrations that did not change significantly during the experimental period (Figure 5). Only 1 animal in the poly C PS-ON-treated group (n = 7) and 2 in the poly AC PS-ON-treated group (n = 5) were HCV positive. The remaining mice in both groups of mice were persistently negative. All 7 mice in the poly C PO-ON-treated mice (100%) and 14 of 15 untreated mice (normal saline placebo) were HCV positive (93%). The *P* value was statistically significance between the PS-ON- and PO-ON-treated groups ($P < .05$). To rule out the possibility that these protected mice were not intrinsically resistant to HCV infection despite robust human hepatocytes engraftment, some of them were rechallenged with infectious HCV inoculum several weeks later. They all became infected, supporting the specific inhibitory effect of APs on de novo HCV infection in this in vivo model.

Discussion

Current therapy for hepatitis C is based on peginterferon and ribavirin. However, the therapy is only effective in approximately half of the patients, and there is little option to those who fail current therapy. Recent advances in the development of small molecule inhibitors targeting the viral-encoded enzymes showed promise,[27] but viral resistance to these drugs is a major clinical issue because HCV is highly variable with rapid viral proliferation and low-fidelity replication. Phosphorothiate modification of oligonucleotides was initially designed to reduce enzymatic degradation. This modification also increases the hydrophobicity of the phosphodiester backbone and thus imparts an amphipathic character to the oligonucleotide polymer.[28] Recent studies showed that

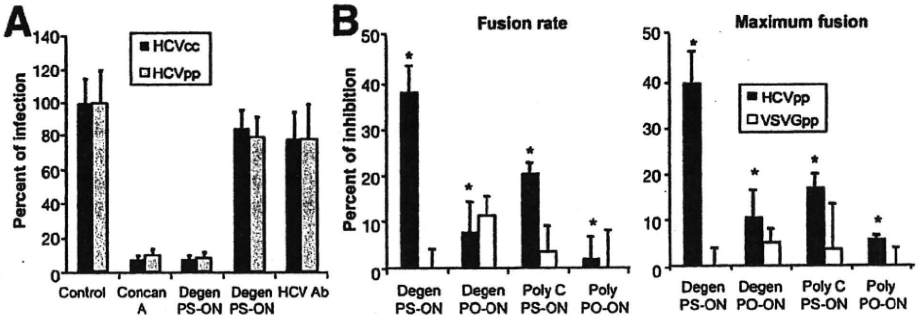

Figure 4. Effects of PS-ON on HCV viral entry. (*A*) Hep3B cells were incubated with HCVpp at 4°C for 1 hour to bind the virus and washed to remove the unbound virus. Cells were then incubated with fresh culture medium containing 25 nmol/L concanamycin A, 100 nmol/L PS-ON, 100 nmol/L PO-ON, or 25 μg/mL (total concentration) AP33+ALP98 monoclonal antibodies at 37°C for 16 hours. The luciferase activities were determined 24 hours later. Results are shown as percentages of infection + SD. (*B*) Fusion assay was performed with HCVpp or VSVGpp in the presence of PS-ON (degenerate or poly C) or the PO-ON controls. The results are expressed as mean percentages (means + SD) of inhibition of either the fusion rate at the origin of the fusion kinetics (*left panel*) or the maximum fusion of the curve at 500 S (*right panel*) relative to incubation in the absence of the compounds. The fusion curves are shown in Supplementary Figure 4. *$P < .05$ comparing the PS-ON and the corresponding PO-ON in the HCVpp fusion assay.

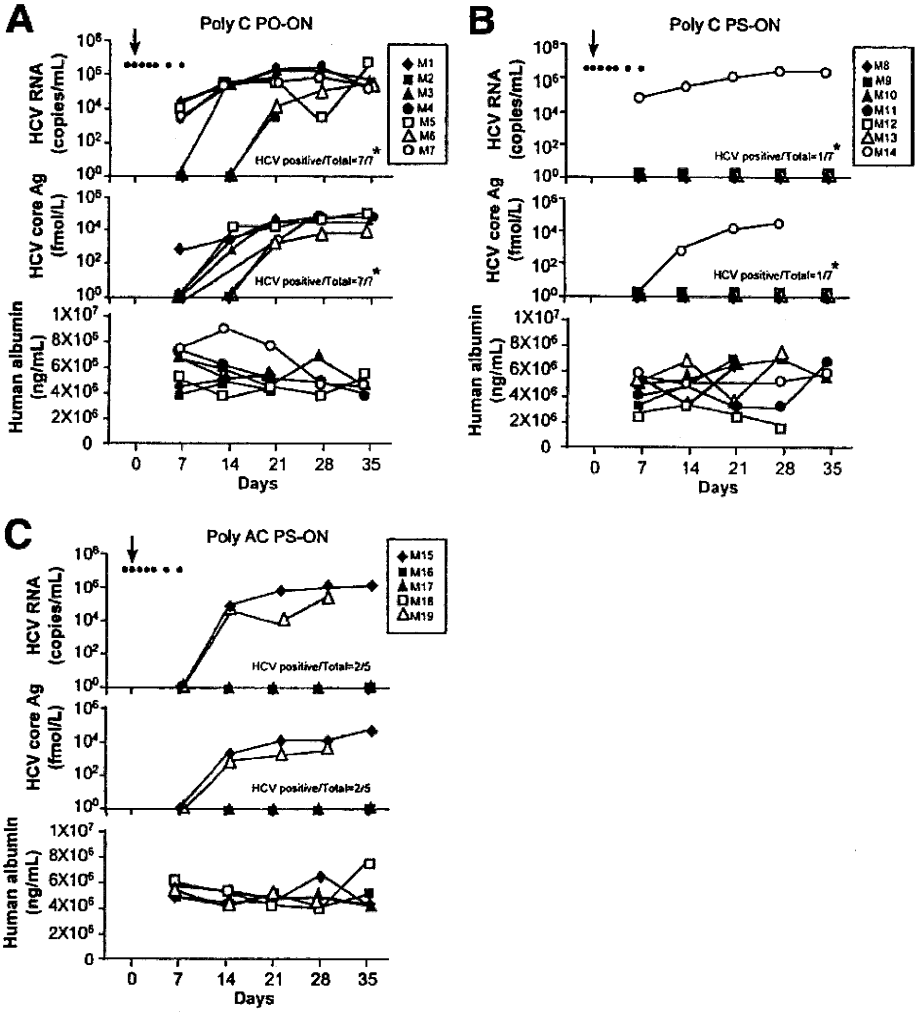

Figure 5. Effects of PS-ON on HCV infection in vivo. Human hepatocytes-transplanted uPA/SCID mice were treated intraperitoneally with 10 mg/kg of PS-ON (poly C) (n = 7) or (poly AC) (n = 5) on days −1, 0, 1, 3, 5, and 7 (indicated by *dots*). The corresponding control PO-ON (poly C) was also tested (n = 7). A fourth group of mice did not receive any compounds (n = 15). The mice were intravenously inoculated on day 0 with HCV patient serum containing 3.9×10^3 copies of HCV genotype 1b (indicated by *arrow*). Serum samples were obtained on days 0 (prior to HCV inoculation), 7, 14, 21, 28, and 35 for HCV RNA and human albumin determination. HCV core antigen was also measured and showed the same results as the HCV RNA determination.

the amphipathic PS-ONs have a sequence-independent antiviral activity against HIV-1 and other viruses,[14,29] suggesting that these compounds may exhibit a broad-spectrum antiviral activity.

Our data showed that PS-ON blocked HCV infection in the HCVcc and HCVpp systems in a similarly dose-dependent manner, with 50% inhibitory concentration in the nanomolar range. PS-ON had no effect on infection of VSVGpp (an enveloped RNA virus with mechanism of viral entry distinct from type I and II fusion) or adenovirus (a nonenveloped DNA virus). The amphipathic nature of PS-ON is crucial for its anti-HCV property because PS-ON analogs lacking the amphipathicity are inactive. Polynucleotides are polyanions, a class of compounds that have been shown to interfere with a variety of viral infections.[30,31] However, our data showed clearly that the polyanionic nature is not relevant to the PS-ON inhibitory activity because the control PO-ON is not active in HCV inhibition. Furthermore, the inhibitory effect of PS-ON could not be explained by the increased stability of the phosphorothioation because the control PO-ON has the 2′-O-methyl modification that also stabilizes the oligonucleotides.[14,23]

The inhibitory activity of APs is sequence independent but length dependent. The degenerate APs were equally effective as the homo- and heteropolymeric sequences, with the exception of poly A and G, which can form unique polypurine quartet structures in solution.[32] The minimal length of PS-ON required for potent inhibitory activities is 40mer, which appears to be the same for all active PS-ON compounds. This length-specific requirement may indicate a critical structural feature of the HCV entry process that is susceptible to these compounds. Although the degenerate PS-ON may contain CpG motif, the other hetero- and homopolymer PS-ONs tested herein are devoid of CpG motifs. The comparable antiviral activity of these compounds to the degenerate PS-ON demonstrates that the antiviral activity is not mediated by the potential CpG-mediated induction of interferon. Furthermore, Huh7.5 cells express very little or none of the cell surface toll-like receptors involved in recognition of nucleic acid-based motifs,[33] and we did

not observe any production of endogenous type I interferons in cells exposed to either PS-ON or PO-ON.

The inhibitory activity of PS-ON appears to target the postbinding and prereplication stage and possibly at the fusion step of HCV infection. The fusion process appears to be structurally conserved among many enveloped viruses and can be classified into types I and II.[34] The type I membrane fusion is exemplified by the influenza and HIV-1 via hemagglutinin and gp41, respectively. The type II fusion includes the alpha-viruses and flaviviruses.[34-36] It has been proposed that HCV uses a type II fusion process because of its similarity to flaviviruses.[37] Our recent study suggests that HCV and flaviviruses are indeed structurally similar.[38] It is conceivable that the fusion process of HCV may be susceptible to inhibition by the amphipathic structure of PS-ON, but further confirmation is necessary. HCV entry has been shown to occur via receptor-mediated endocytosis and is sensitive to lysosomotropic agents and inhibitors of vacuolar ATPases.[39] The finding that PS-ON acts at the postbinding step like concanamycin A and bafilomycin A1, which are potent inhibitors of the vacuolar ATPases, supports this hypothesis. Furthermore, all HCV genotypes appeared to be susceptible to the APs equally, suggesting that the process involved is highly conserved.

HCV entry involves multiple cellular factors, such as CD81, SR-B1, Claudin-1, heparin sulfate, DC-SIGN, and L-SIGN, and possibly LDL receptor.[5-10,31] CD81 and Claudin-1 have been postulated to act on the postbinding step.[6,40] SR-B1 is likely involved in an early viral entry step to the cells. Its interaction with apolipoproteins and cholesterol transfer property appear to be important for viral entry,[41] possibly at the level of membrane fusion.[42] The overall mechanism of HCV entry is complex and involves multiple factors and steps. The APs likely interact with 1 of these essential steps to abort HCV entry. The unique inhibitory effect of the APs on HCV infection makes it a valuable reagent to study the molecular pathway of HCV entry. The APs can also be developed as a molecular probe to image and dissect biochemically this complex process.

Our study demonstrates that APs are potent inhibitors of HCV infection. APs are equally effective against all HCV genotypes and can inhibit de novo HCV infection in the human hepatocyte-transplanted uPA/SCID mouse model. This approach has the advantage of a novel and highly conserved target mechanism that is distinct from the small molecule inhibitors being developed clinically as well as the well-established pharmacology of antisense-based nucleic acid molecules in clinical trials. The effectiveness of this class of compounds in blocking de novo HCV infection supports its value in liver transplantation to prevent reinfection, which occurs invariably and presents a major problem for the management of these patients.[43] So far, prophylactic reagents based on neutralizing antibodies have been disappointing in clinical trials of liver transplantation.[44] Our studies illustrate the promise of this class of compounds as a potent antiviral against HCV and support its further development in the therapy of hepatitis C.

Supplementary Data

Note: To access the supplementary material accompanying this article, visit the online version of *Gastroenterology* at www.gastrojournal.org, and at doi: 10.1053/j.gastro.2009.04.048.

References

1. Liang TJ, Rehermann B, Seeff LB, et al. Pathogenesis, natural history, treatment, and prevention of hepatitis C. Ann Intern Med 2000;132:296–305.
2. Feld JJ, Hoofnagle JH. Mechanism of action of interferon and ribavirin in treatment of hepatitis C. Nature 2005;436:967–972.
3. Pawlotsky JM. Therapy of hepatitis C: from empiricism to eradication. Hepatology 2006;43:S207–S220.
4. Smith AE, Helenius A. How viruses enter animal cells. Science 2004;304:237–242.
5. Bartosch B, Dubuisson J, Cosset FL. Infectious hepatitis C virus pseudo-particles containing functional E1-E2 envelope protein complexes. J Exp Med 2003;197:633–642.
6. Evans MJ, von Hahn T, Tscherne DM, et al. Claudin-1 is a hepatitis C virus co-receptor required for a late step in entry. Nature 2007;446:801–805.
7. Hsu M, Zhang J, Flint M, et al. Hepatitis C virus glycoproteins mediate pH-dependent cell entry of pseudotyped retroviral particles. Proc Natl Acad Sci U S A 2003;100:7271–7276.
8. Lindenbach BD, Evans MJ, Syder AJ, et al. Complete replication of hepatitis C virus in cell culture. Science 2005;309:623–626.
9. Lozach PY, Lortat-Jacob H, de Lacroix de Lavalette A, et al. DC-SIGN and L-SIGN are high affinity binding receptors for hepatitis C virus glycoprotein E2. J Biol Chem 2003;278:20358–20366.
10. Scarselli E, Ansuini H, Cerino R, et al. The human scavenger receptor class B type I is a novel candidate receptor for the hepatitis C virus. EMBO J 2002;21:5017–5025.
11. Bartosch B, Vitelli A, Granier C, et al. Cell entry of hepatitis C virus requires a set of co-receptors that include the CD81 tetraspanin and the SR-B1 scavenger receptor. J Biol Chem 2003; 278:41624–41630.
12. Koutsoudakis G, Kaul A, Steinmann E, et al. Characterization of the early steps of hepatitis C virus infection by using luciferase reporter viruses. J Virol 2006;80:5308–5320.
13. Rusconi S, Scozzafava A, Mastrolorenzo A, et al. An update in the development of HIV entry inhibitors. Curr Top Med Chem 2007; 7:1273–1289.
14. Vaillant A, Juteau JM, Lu H, et al. Phosphorothioate oligonucleotides inhibit human immunodeficiency virus type 1 fusion by blocking gp41 core formation. Antimicrob Agents Chemother 2006;50:1393–1401.
15. Wakita T, Pietschmann T, Kato T, et al. Production of infectious hepatitis C virus in tissue culture from a cloned viral genome. Nat Med 2005;11:791–796.
16. Lavillette D, Tarr AW, Voisset C, et al. Characterization of host-range and cell entry properties of the major genotypes and subtypes of hepatitis C virus. Hepatology 2005;41:265–274.
17. Owsianka A, Tarr AW, Juttla VS, et al. Monoclonal antibody AP33 defines a broadly neutralizing epitope on the hepatitis C virus E2 envelope glycoprotein. J Virol 2005;79:11095–11104.
18. Kato T, Date T, Miyamoto M, et al. Detection of anti-hepatitis C virus effects of interferon and ribavirin by a sensitive replicon system. J Clin Microbiol 2005;43:5679–5684.

19. Nanda SK, Herion D, Liang TJ. The SH3 binding motif of HCV (corrected) NS5A protein interacts with Bin1 and is important for apoptosis and infectivity. Gastroenterology 2006;130:794–809.
20. Triyatni M, Saunier B, Maruvada P, et al. Interaction of hepatitis C virus-like particles and cells: a model system for studying viral binding and entry. J Virol 2002;76:9335–9344.
21. Lavillette D, Bartosch B, Nourrisson D, et al. Hepatitis C virus glycoproteins mediate low pH-dependent membrane fusion with liposomes. J Biol Chem 2006;281:3909–3917.
22. Tateno C, Yoshizane Y, Saito N, et al. Near completely humanized liver in mice shows human-type metabolic responses to drugs. Am J Pathol 2004;165:901–912.
23. Lamond AI, Sproat BS. Antisense oligonucleotides made of 2'-O-alkylRNA: their properties and applications in RNA biochemistry. FEBS Lett 1993;325:123–127.
24. Steinmann D, Barth H, Gissler B, et al. Inhibition of hepatitis C virus-like particle binding to target cells by antiviral antibodies in acute and chronic hepatitis C. J Virol 2004;78:9030–9040.
25. Baumert TF, Vergalla J, Satoi J, et al. Hepatitis C virus-like particles synthesized in insect cells as a potential vaccine candidate. Gastroenterology 1999;117:1397–1407.
26. Wellnitz S, Klumpp B, Barth H, et al. Binding of hepatitis C virus-like particles derived from infectious clone H77C to defined human cell lines. J Virol 2002;76:1181–1193.
27. Pawlotsky JM, Chevaliez S, McHutchison JG. The hepatitis C virus life cycle as a target for new antiviral therapies. Gastroenterology 2007;132:1979–1998.
28. Agrawal S, Tang JY, Brown DM. Analytical study of phosphorothioate analogues of oligodeoxynucleotides using high-performance liquid chromatography. J Chromatogr 1990;509:396–399.
29. Lee AM, Rojek JM, Gundersen A, et al. Inhibition of cellular entry of lymphocytic choriomeningitis virus by amphipathic DNA polymers. Virology 2008;372:107–117.
30. Moulard M, Lortat-Jacob H, Mondor I, et al. Selective interactions of polyanions with basic surfaces on human immunodeficiency virus type 1 gp120. J Virol 2000;74:1948–1960.
31. Barth H, Schafer C, Adah MI, et al. Cellular binding of hepatitis C virus envelope glycoprotein E2 requires cell surface heparan sulfate. J Biol Chem 2003;278:41003–41012.
32. Kim J, Cheong C, Moore PB. Tetramerization of an RNA oligonucleotide containing a GGGG sequence. Nature 1991;351:331–332.
33. Preiss S, Thompson A, Chen X, et al. Characterization of the innate immune signalling pathways in hepatocyte cell lines. J Viral Hepat 2008;15:888–900.
34. Kielian M, Rey FA. Virus membrane-fusion proteins: more than one way to make a hairpin. Nat Rev Microbiol 2006;4:67–76.
35. Kielian M. Class II virus membrane fusion proteins. Virology 2006;344:38–47.
36. Lescar J, Roussel A, Wien MW, et al. The fusion glycoprotein shell of Semliki Forest virus: an icosahedral assembly primed for fusogenic activation at endosomal pH. Cell 2001;105:137–148.
37. Yagnik AT, Lahm A, Meola A, et al. A model for the hepatitis C virus envelope glycoprotein E2. Proteins 2000;40:355–366.
38. Yu X, Qiao M, Atanasov I, et al. Cryo-electron microscopy and three-dimensional reconstructions of hepatitis C virus particles. Virology 2007;367:126–134.
39. Tscherne DM, Jones CT, Evans MJ, et al. Time- and temperature-dependent activation of hepatitis C virus for low-pH-triggered entry. J Virol 2006;80:1734–1741.
40. Cormier EG, Tsamis F, Kajumo F, et al. CD81 is an entry coreceptor for hepatitis C virus. Proc Natl Acad Sci U S A 2004;101:7270–7274.
41. Bartosch B, Verney G, Dreux M, et al. An interplay between hypervariable region 1 of the hepatitis C virus E2 glycoprotein, the scavenger receptor BI, and high-density lipoprotein promotes both enhancement of infection and protection against neutralizing antibodies. J Virol 2005;79:8217–8229.
42. Dreux M, Boson B, Ricard-Blum S, et al. The exchangeable apolipoprotein ApoC-I promotes membrane fusion of hepatitis C virus. J Biol Chem 2007;282:32357–32369.
43. Samuel D, Bizollon T, Feray C, et al. Interferon-α 2b plus ribavirin in patients with chronic hepatitis C after liver transplantation: a randomized study. Gastroenterology 2003;124:642–650.
44. Schiano TD, Charlton M, Younossi Z, et al. Monoclonal antibody HCV-AbXTL68 in patients undergoing liver transplantation for HCV: results of a phase 2 randomized study. Liver Transpl 2006;12:1381–1389.

Received December 28, 2008. Accepted April 16, 2009.

Reprint requests

Address requests for reprints to: T. Jake Liang, MD, LDB/NIDDK/NIH, Bldg 10-9B16, 10 Center Dr, Bethesda, Maryland. e-mail: JakeL@bdg10.niddk.nih.gov; fax: (301) 402-0491.

Acknowledgments

The authors thank Charles Rice, Robert Purcell, Jens Bukh, and Thomas Baumert for providing various valuable reagents.

Conflicts of interest

The authors diclose the following: J.-M.J. and A.V. are employees of REPLICor, Inc. The remaining authors disclose no conflicts.

Funding

Supported in part by the Intramural Research Program of the National Institute of Diabetes and Digestive and Kidney Diseases, NIH, and a NIH Cooperative Research and Development Agreement (DK-06-0367) between NIDDK and REPLICor, Inc.

nature genetics

A genome-wide association study identifies variants in the *HLA-DP* locus associated with chronic hepatitis B in Asians

Yoichiro Kamatani[1,2], Sukanya Wattanapokayakit[3], Hidenori Ochi[4,5], Takahisa Kawaguchi[4], Atsushi Takahashi[4], Naoya Hosono[4], Michiaki Kubo[4], Tatsuhiko Tsunoda[4], Naoyuki Kamatani[4], Hiromitsu Kumada[6], Aekkachai Puseenam[7], Thanyachai Sura[7], Yataro Daigo[1,2], Kazuaki Chayama[4,5], Wasun Chantratita[8], Yusuke Nakamura[1,4] & Koichi Matsuda[1]

Chronic hepatitis B is a serious infectious liver disease that often progresses to liver cirrhosis and hepatocellular carcinoma; however, clinical outcomes after viral exposure vary enormously among individuals[1]. Through a two-stage genome-wide association study using 786 Japanese chronic hepatitis B cases and 2,201 controls, we identified a significant association of chronic hepatitis B with 11 SNPs in a region including *HLA-DPA1* and *HLA-DPB1*. We validated these associations by genotyping two SNPs from the region in three additional Japanese and Thai cohorts consisting of 1,300 cases and 2,100 controls (combined $P = 6.34 \times 10^{-39}$ and 2.31×10^{-38}, OR = 0.57 and 0.56, respectively). Subsequent analyses revealed risk haplotypes (*HLA-DPA10202-*DPB1**0501 and *HLA-DPA1**0202-*DPB1**0301, OR = 1.45 and 2.31, respectively) and protective haplotypes (*HLA-DPA1**0103-*DPB1**0402 and *HLA-DPA1**0103-*DPB1**0401, OR = 0.52 and 0.57, respectively). Our findings show that genetic variants in the *HLA-DP* locus are strongly associated with risk of persistent infection with hepatitis B virus.**

Chronic hepatitis B is one of the most common infectious liver diseases caused by hepatitis B virus (HBV). HBV infection shows a marked regional diversity and is very prevalent in the Asia-Pacific region; HBsAg seropositivity rates are as high as 5–12% in Thai and China, but as low as 0.2–0.5% in North America and Europe[2]. It is estimated that, at present, more than 400 million people worldwide are chronically infected with HBV, and nearly 60% of liver cancers are considered to be related to chronic hepatitis B and subsequent liver cirrhosis[3]. Most HBV carriers are considered to have been infected through maternal transmission in the neonatal period or infancy, particularly in Japan[4]. Although some HBV carriers spontaneously eliminate the virus, 2–10% of individuals with chronic hepatitis B are estimated to develop liver cirrhosis every year, and a subset of these individuals suffer from liver failure or hepatocellular carcinoma[1]. Because clinical outcomes after exposure to HBV are highly variable, identification of genetic and environmental factors that are related to progression of HBV-induced liver diseases is critical.

Several epidemiological factors such as age at infection, sex, chronic alcohol abuse[5] and co-infection with other hepatitis viruses[6] were suspected to affect viral persistence. In addition, a twin study in Taiwan indicated that host genetic background influences infection outcome[7]. Although genetic variants in *IFNG*, *TNF*, *VDR*, *ESR1* and several *HLA* loci were shown to associate with chronic hepatitis B[8–12], none of the associations has been proven to be conclusive. To identify disease-predisposing variants, we carried out a two-stage association study for chronic hepatitis B using genome-wide SNPs as genetic markers.

Characteristics of each cohort group are shown in **Supplementary Table 1** online. We carried out a two-stage genome-wide association approach as described in the Methods. In the first stage, we genotyped 179 Japanese individuals with chronic hepatitis B and 934 control individuals using Illumina HumanHap550 BeadChip (**Fig. 1a**). For the second stage, we selected the top 12,000 SNPs that had the smallest *P* values on the basis of minimum *P* value considering three genetic models: allelic, dominant or recessive. Analysis of an independent set of 607 cases and 1,267 controls using these sub-selected SNPs showed 11 SNPs to be significantly associated ($P = 3.62 \times 10^{-8} \sim 1.16 \times 10^{-13}$) with chronic hepatitis B after Bonferroni correction (**Fig. 1b** and **Supplementary Table 2** online). Application of the Cochrane-Armitage

[1]Laboratory of Molecular Medicine, Human Genome Center, Institute of Medical Science, the University of Tokyo, Tokyo, Japan. [2]Department of Medical Genome Sciences, Graduate School of Frontier Sciences, the University of Tokyo, Tokyo, Japan. [3]Medical Genetic Section, National Institute of Health, Department of Medical Sciences, Ministry of Public Health, Nonthaburi, Thailand. [4]Center for Genomic Medicine, RIKEN, Kanagawa, Japan. [5]Department of Medicine and Molecular Science, Division of Frontier Medical Science, Programs for Biomedical Research, Graduate School of Biomedical Sciences, Hiroshima University, Hiroshima, Japan. [6]Department of Hepatology, Toranomon Hospital, Tokyo, Japan. [7]Department of Medicine, Faculty of Medicine and [8]Virology and Molecular Microbiology Unit, Department of Pathology, Faculty of Medicine, Ramathidi Hospital, Mahidol University, Bangkok, Thailand. Correspondence should be addressed to Y.N. (yusuke@ims.u-tokyo.ac.jp).

Received 10 November 2008; accepted 16 January 2009; published online 6 April 2009; doi:10.1038/ng.348

test to all the tested SNPs indicated that the genetic inflation factor lambda was 1.02 for the second stage (**Supplementary Fig. 1a** online), implying a low possibility of false positive associations due to population stratification. All 11 SNPs are located within or around the *HLA-DPA1* and *HLA-DPB1* locus (**Fig. 2**). We also conducted age- and sex-adjusted analysis using a logistic regression model, and confirmed similar association after adjustment (data not shown).

To validate the result of the discovery-phase analysis, we carried out replication analyses using three independent cohorts. We selected the most or second-most strongly associated SNPs from each *HLA-DP* locus (rs9277535 on *HLA-DPB1* and rs3077 on *HLA-DPA1*, respectively), as we failed to design a Taqman or Invader probe for rs2395309 on *HLA-DPA1*. We first examined two independent sets of Japanese case–control samples comprising 274 cases and 274 controls (age-, sex- and alcohol consumption–matched cohort from BioBank Japan) as well as 718 cases and 1,280 controls. We found significant associations at two SNP loci in both studies ($P = 1.06 \times 10^{-16} \sim 1.96 \times 10^{-6}$; **Table 1**). We also genotyped 308 individuals with chronic hepatitis B and 546 healthy controls in Thailand, and further confirmed the association at the two loci, rs3077 ($P = 6.53 \times 10^{-6}$) and rs9277535 ($P = 6.52 \times 10^{-8}$).

To combine these studies, we conducted a meta-analysis with a fixed-effects model using the Mantel-Haenszel method. As shown in **Table 1** and **Supplementary Figure 1b**, the odds ratios (OR) were quite similar across the four studies (the second stage of GWAS and three replication studies) and no heterogeneity was observed. Mantel-Haenszel *P* values for independence were 2.31×10^{-38} for rs3077 (OR = 0.56, 95% confidence interval (CI) = 0.51–0.61), and 6.34×10^{-39} for rs9277535 (OR = 0.57, 95% CI = 0.52–0.62).

The 11 SNPs showing significant associations are located within a 50-kb region including *HLA-DPA1* and *HLA-DPB1* (**Fig. 2**). Although the *HLA* region is known to show extensive linkage disequilibrium (LD) spanning over 7 Mb, the LD block including these 11 SNPs (surrounded by a bold line in **Fig. 2a**) was not in strong LD with the other *HLA* loci. In accordance with the extent of LD, only SNPs around the *HLA-DPA1* and *HLA-DPB1* genes showed very strong associations with chronic HBV (surrounded by a bold line in **Fig. 2b**), and SNPs outside of this particular LD block did not have significant association.

HLA-DPA1 and *HLA-DPB1* encode the HLA-DP α and β chains, respectively. HLA-DPs belong to the HLA class II molecules that form heterodimers on the cell surface and present antigens to CD4-positive T lymphocytes. HLA-DPs are highly polymorphic, especially in exon 2, which encodes antigen-binding sites. We thus considered that the association of these SNPs with chronic HBV might reflect variations in antigen-binding sites that might affect the immune response to HBV. We genotyped *HLA-DPA1* and *HLA-DPB1* alleles by direct sequencing of exon 2 (cases at second stage and controls at first stage) and found significant association of chronic hepatitis B with *HLA-DPA1**0103, *DPA1**0202, *DPB1**0402 and *DPB1**0501 ($P = 2.93 \times 10^{-11}$, 4.45×10^{-8}, 2.27×10^{-7} and 6.98×10^{-7}, respectively; **Supplementary Table 3** online). Because sequence variants in exon 2 of *HLA-DPA1* and *HLA-DPB1* could be linked to individual nucleotide variants, we inferred haplotypes using the 11 SNPs and variants in exon 2, and found very strong LD among them (**Supplementary Fig. 2**

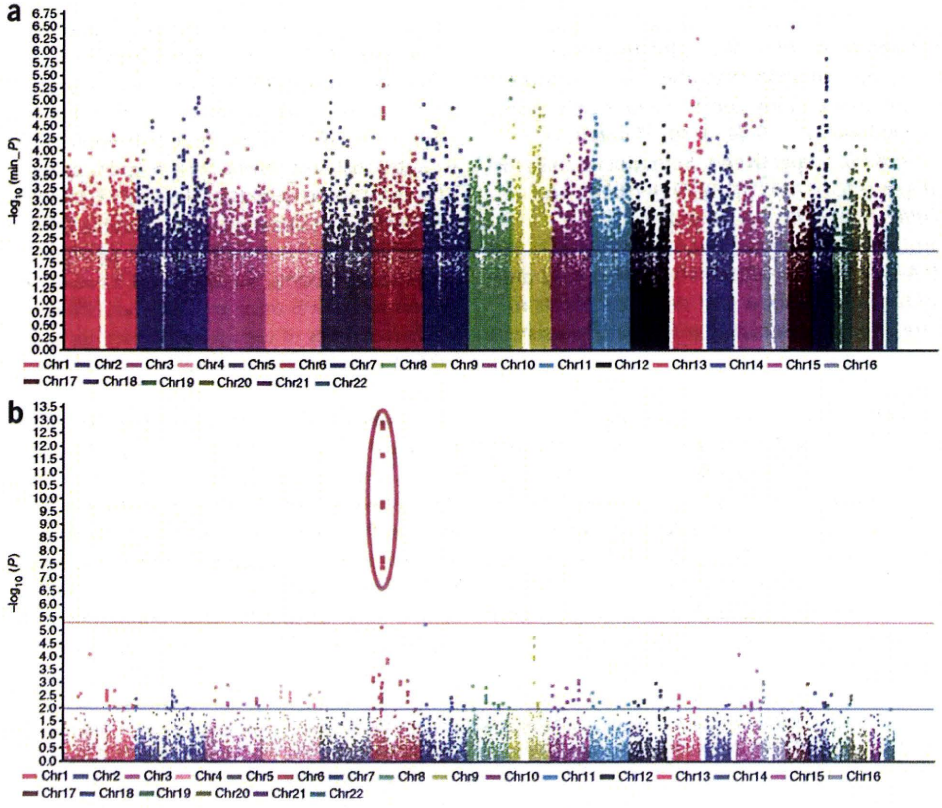

Figure 1 Results from a two-stage genome-wide association study. (**a**) $-\log_{10}$ *P* value plot at the first stage. Each *P* value is the minimum of Fisher's exact tests for three models: dominant, recessive and allele frequency model. (**b**) $-\log_{10}$ *P* value plot at the second stage. *P* values were calculated by 1-d.f. Cochrane-Armitage trend test. The large dots circled by red on the chromosome 6 showed significant associations ($P < 5.06 \times 10^{-6}$) with chronic hepatitis B.